CHALMERS
UNIVERSITY OF TECHNOLOGY

Dynamic simulations of an oil and gas well stream

A study of the dynamic behaviour of the flow in a subsea pipeline and its impact on downstream equipment

Master's thesis in Innovative and Sustainable Chemical Engineering

LINNEA JÖRGNER
ERIK RILBY

Department of Chemistry and Chemical Engineering
CHALMERS UNIVERSITY OF TECHNOLOGY
Gothenburg, Sweden 2016

Master's thesis 2016

Dynamic simulations of an oil and gas well stream

A study of the dynamic behaviour of the flow in a subsea pipeline and its impact on downstream equipment

Linnea Jörgner
Erik Rilby

CHALMERS
UNIVERSITY OF TECHNOLOGY

Department of Chemistry and Chemical Engineering
Division of Chemical Engineering
Chalmers University of Technology
Gothenburg, Sweden 2016

Dynamic simulations of an oil and gas well stream
A study of the dynamic behaviour of the flow in a subsea pipeline and its impact on downstream equipment

LINNEA JÖRGNER
ERIK RILBY

Supervisor: Johan Liedman, Reinertsen Sverige AB
Examiner: Gunnar Eriksson, Chemistry and Chemical Engineering

Master's Thesis 2016
Department of Chemistry and Chemical Engineering
Division of Chemical Engineering
Chalmers University of Technology
SE-412 96 Gothenburg
Telephone +46 31 772 1000

Typeset in LaTeX
Gothenburg, Sweden 2016

Abstract

Today, offshore production of oil and gas constitutes a large share of the total oil and gas production. Wells where the oil and gas are extracted can be located close to the production platform or several kilometers away and connected through flowlines. To safely extract oil and gas, dimensioning and evaluating of process and safety equipment are highly prioritised. Modeling and simulations are helpful for providing accurate estimations of the flow behaviour. The subsea and topside system are often treated separately when constructing modeling and simulations. Thus the simulation of the production facility does not account for the dynamic behaviour of the subsea piping. In this thesis the dynamic effect of the subsea part has been included to see its effect on the downstream equipment. An existing satellite field in the North Sea was chosen for validation of the model. The model was formulated using the process modeling tool Aspen HYSYS. Three dynamic scenarios were investigated: a shut-down, a start-up and a choke collapse. Cases with different model complexity were formulated for the choke collapse scenario. Results showed that some dynamic behaviour were not seen in the formulated model for slow dynamic events. It was also seen that by including parts of the subsea system, to some extension, the dynamic effects of the topside equipment can be evaluated more accurately.

Keywords: dynamic, simulation, oil, gas, subsea, flowline, riser, offshore, choke collapse, HYSYS.

Acknowledgements

It all started during a snowy morning in January. During the night it had fallen about 20 cm of snow which resulted in cancelled trams and buses. We both had to walk, as everyone did that morning, through Gothenburg down to the office at Gullbergsvass. Thereafter, during the course of six months as our work progressed the spring came and went and finally reached in to the summer, like the maturing of our knowledge and experience. During this time at Reinertsen, we have learned a lot. We are grateful for the opportunity we were given to conduct our thesis work at the office in Gothenburg. We want to thank Johan, our supervisor, who has helped us with everything from finding documentation to proofreading and support. We also want to thank Bernt and Lennart for taking the time to help us and with their expertise discussing results and course of action. Of course we want to thank all the people at the process department at Reinersten, which have included us and made us feel like a part of the group from the very first day. We want to thank our examiner Gunnar Eriksson at Chalmers, that has helped us with administration, software licenses and giving us a lot of freedom in the execution of the work. Of course we want to thank all our friends and families for their patience and support.

Linnea Jörgner & Erik Rilby, Gothenburg, June 2016

Table of Contents

List of Figures

List of Tables

List of Symbols

Greek letters

ν	Molar volume

Latin letters

a	Empirical correlation constant
b	Empirical correlation constant
C_V	Flow coefficient for valves
G	Specific gravity
n	Number of moles of gas
P	Absolute pressure
R	The universal gas constant
S	Standard conditions at 15 °C and 1 bar
T	Absolute temperature

List of Abbreviations

EOS	Equation of state
GOR	Gas to oil ratio
PSV	Pressure safety valve
PVT	Pressure, volume and temperature
SSIV	Subsea isolation valve
WC	Watercut

1 Introduction

As the worldwide energy demand has increased during the last decades the energy production from the offshore oil and gas industry has grown to meet these demands [1]. To safely operate and handle the volatile substances in the harsh offshore environment extensive and accurate evaluations of the equipment and systems has to be performed.

1.1 Historical Background

Offshore oil production began in 1896 in California, United States [2]. Though, it was not until after World War II the U.S. oil companies were taking larger steps in exploitation of offshore resources. In 1947 the company Kerr-McGee completed the first oil rig in the Gulf of Mexico, which today is seen as the start of the offshore industry. The rig stood on the seabed with a water depth of 4.6 meters [3]. Since then the offshore industry has gone further out and deeper into the oceans. Due to technical advancement within the business by 2010 the deepest oil rigs were operating approximately at a water depth of 12 000 feet (∼3700 meters) [2].

In the North Sea findings of natural gas resources were made and exploited during the 1960's. During the 1970's oil and gas fields were first found. The first oil and gas findings were made in what is now called the Ekofisk and Forties fields. Exploitation of these fields, and the entire North Sea, would come as a great challenge for companies. The harsh environment with severe storms, tidal waves and cold weather needed great research and development of new techniques. [4, 5]

The world's energy demand is continuing to be high and the oil and gas production industry is still a considerable contributor to satisfy a great part of this demand. With an increasing energy consumption in the emerging countries, the demand for energy produced from oil and gas is considered of many experts to be high at least in the nearest future [2]. In the search for new reservoirs the offshore drilling proceeds to move deeper out in the sea and to more distant places with larger inaccessibility. Hence, offshore oil and gas production equipment need to be continuously developed and improved. Therewith, existing platforms need to be modified to maintain the required production capacity and still be taking all safety aspects into concern. [1]

1.2 Overview of offshore oil and gas production

Offshore oil and gas production units can be divided in some major groupings: wells, platforms and pipelines. These groups of units can then be divided further. Following the product flow direction, the production starts at the well. The well head is located over a reservoir, which is an oil and gas formation under the seabed. The well is drilled commonly using a drill located on a platform. Wells can be drilled in vertical, declined or horizontal direction into the formation. If the pressure difference between the well and topside production is significant the oil and gas will flow without no need for assistance. However, if the pressure gradient is not sufficient to lift the oil and gas out of the well additional pumping or work has to be added. [6]

When the fluid mixture of water, oil and gas leaves the well it is transported through a subsea flowline, i.e. a pipeline from the well to the surface platform. The pipeline can be connected either to a well platform and then to a processing platform, or directly to a processing platform. It is common that wells are located far away from the processing platform, thus, the length of the pipeline can be up to several kilometers long. [6] Platforms are established for different purposes. Platforms can be built and moved solely for drilling of new wells, for connection of wells, for oil and gas processing or to handle multiple of these assignments. Platforms can, in shallow water, be standing on the seabed. For deeper water, and for possibility to move the rig easily, the rig is commonly floating. Several solutions and designs of platforms exist. On board the platform product pipelines are collected and connected to a manifold before entering the separation and processing stage. The pipelines from each well can be opened or closed through a choke located upstream, before the manifold. [6, 7]

1.3 Scope of Thesis

Offshore oil and gas pipelines often need to handle high pressures and flow rates to transport the multiphase fluid to the platform in a controlled way. The system contains safety equipment such as valves and controllers to prevent incidents and accidents. The modelling of offshore systems is often done with steady state assumptions. However, it is of great interest to simulate a transient behaviour of these kinds of systems to be able to make more accurate assessments of what would happen in real case scenarios.

1.3.1 Objective

The objective of this thesis is to examine the dynamic behaviour of an oil and gas subsea flowline and its effects on downstream equipment. One of the purposes is

to study different specific events such as start-up, shut-down and choke collapse. This will be achieved by modelling and simulation of an oil and gas pipeline and connecting process equipment.

In extension to the objective, following questions are planned to be answered in the thesis:

1. *Will dynamic simulations of the subsea system have effects on design and sizing of topside downstream equipment?*

If dynamic simulations can be used in risk assessment, safety margins can be in a more suitable range. Steady state simulations may lead to overestimation or underestimation of sizing of the equipment.

2. *To what extend can the model/models be simplified? For the system to be representable and valid, how coarse can the resolution be?*

As a model is simplified, the less computational cost will be required. This will result in faster simulations which leads to reduced need for resources.

3. *Can an efficient framework for simulations of similar systems be expressed?*

If a generalization of a dynamic model of a pipeline is made, time required for assessment of new simulations may be reduced. This will lead to less time spent on model design choices.

2 Theory

Production of crude oil and natural gas require transport from the reservoir to a production facility. The main process on the production facility is to separate the multiphase mixture into desired products and to make the products suitable for export. Depending on the conditions, multiphase flows show a variable behaviour which can make the transport and production unsteady. To maintain a safe production, and to take possible extreme scenarios into account, equipment such as safety valves need to be installed. In addition, flow assurance is performed to ensure stable production. To evaluate a production process to be built, or future modifications on an existing facility, mathematical modelling and simulations are used. The following sections provide deeper insight of these subjects.

2.1 Oil and gas production and products

As the name implies, two products are exported from an oil and gas production facility; crude oil and natural gas. In order to achieve these two products reservoir fluid is extracted from a well. The reservoir fluid contains a broad mixture of hydrocarbons in gaseous and liquid form which will result in products [6]. The reservoir fluid also contains water and a relative small amount of sand and other solid particles. The amount of water in the reservoir fluid is characterised by the volume flow of water over the volume flow of all liquid at standard conditions, pressure of 1 atm and a temperature of 15°C [6, 8]. This is referred to as water cut (WC). Knowing the ratio between the products is also of importance and is often determined through the so called Gas to Oil Ratio (GOR). GOR is defined as the ratio of gas volume flow over the oil volume flow at standard conditions, $(\frac{Sm^3}{h})/(\frac{Sm^3}{h})$ [6, 9].

2.2 Subsea system design

The subsea system consists of some major subsystems. These subsystems are the well, wellhead, template, production flowline and production riser. These subsystems are hereafter described further.

2.2.1 Well

The subsea well is, roughly simplified, the bore hole to the hydrocarbon reservoir. The well is drilled by a drilling platform or drilling ship. The well can be drilled in fully vertical or be directed in whichever inclination preferred [10]. The bore hole is usually supported by inner walls and includes piping, valves and instrumentation. To retrieve liquid from the well process gas can be injected from the platform through a pipeline into the well to decrease the density of the fluid. This results in a reduced static pressure drop which increases the flowrate. This process is called gas lift [6].

2.2.2 Wellhead

The wellhead is situated on the seabed on top of the well. The wellhead consist of several valves, chemical injectors and metering equipment. The valves and instrument components assembly is commonly called the christmas tree. The wellhead is the connection between the well and the subsea template. [6, 11].

2.2.3 Subsea template

The subsea template (seen in figure 2.1) is the structure which contains the assembly of several ingoing and outgoing pipes, umbilicals, valves and instruments to the well. The template often sits over the wellhead and Christmas tree. The template has another purpose, which is to protect the equipment against collision from e.g. bottom trawling nets or anchors. [11]

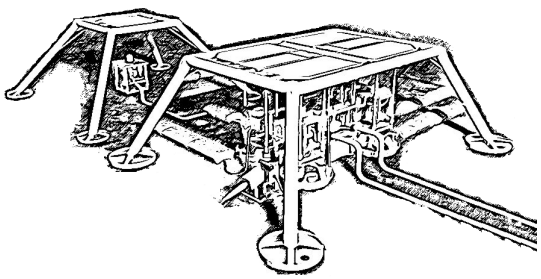

Figure 2.1: Schematic of a subsea template.

2.2.4 Pipeline

The main goal of a pipeline is to transport fluid from one location to another. Offshore industry pipelines have typically following applications: retrieve product from wells/wellheads, transport product from subsea manifolds to processing platforms, transport product between platforms and to transport product to mainland. In choosing and designing a pipeline several aspects have to be considered. What is the intended production rate? How large will the internal and external forces be on the pipeline? How does the routing effects the pipeline? What material should be chosen for the pipeline, both interior and exterior? [7]

Pipelines can be designed in many ways. The most straightforward is a smooth, cylindrical, pipe with an interior wall of metal and a outer casing. Pipelines can be fixed, as previously mentioned, or flexible with some outer plastic or rubber tubing. Pipelines can have internal piping to transport injection chemicals or for heating of the product. [7]

2.3 Topside system design

Offshore production facilities main purpose is to retrieve, process and export product from the connected wells in a safe way. The retrieved fluid goes through several three-phase separation stages. Each gas outlet meets a compressor stage in a compressor train which increases the pressure of the gas before storage or export. If any system or equipment needs to be depressurised hydrocarbons or other chemicals will be burned in the so called flare. The separation and flare systems will be described further in following sections. [12]

2.3.1 Separation and compressor stages

The feed stream that reaches the platform consists of three phases, oil, gas and liquid water. In order to export the products, which is oil and gas, they need to be separated. The separation process aboard a production facility commonly consists of two three-phase separators and one two-phase separator in series. [6, 12] A schematic of a typical setup of separation stages is shown in figure 2.2. Depending on the feed streams pressure when reaching the platform, they can be routed individually to a separator with similar and lower pressure [6].

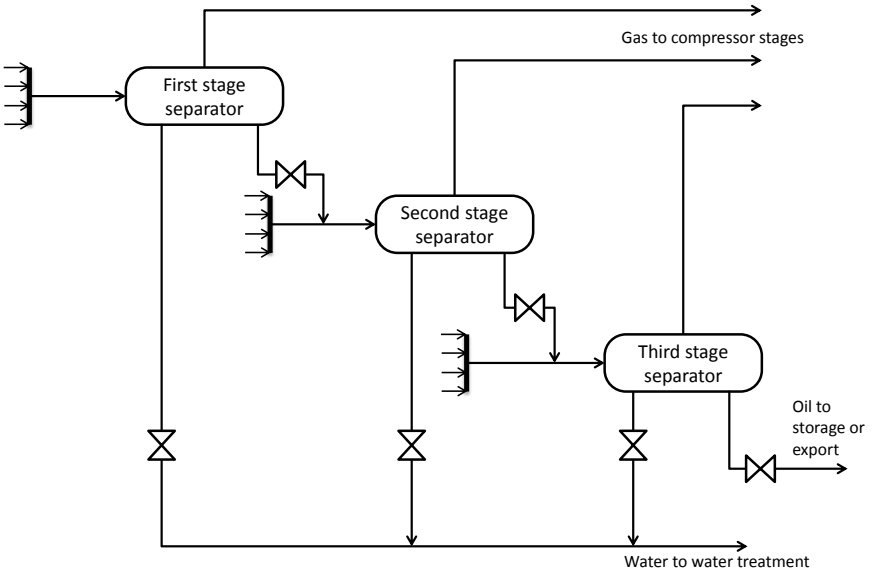

Figure 2.2: Schematic over three stage separation stages.

A schematic of one common setup for a separator stage is shown in figure 2.3. A three-phase separator works mainly through density differences. The multiphase inlet settles and stratifies during the retention time for the fluids in the separator. The gas has the lowest density and due to that it will be located in the top part of the vessel. The oil, which has lower density than water will be located between the gas and water phase. Thus, the gas outlet is mounted in the top of the vessel, the oil outlet in the middle and the water outlet in the bottom. The liquid levels in the vessel are controlled by regulators controlling the flow through valves downstream the liquid outlets. The pressure in the vessel is controlled through control valves and/or regulating the speed of the downstream compressor. Pressure safety valves (PSV) are connected to the separator to release gas to the flare system to prevent overpressure in the separator. [12, 13]

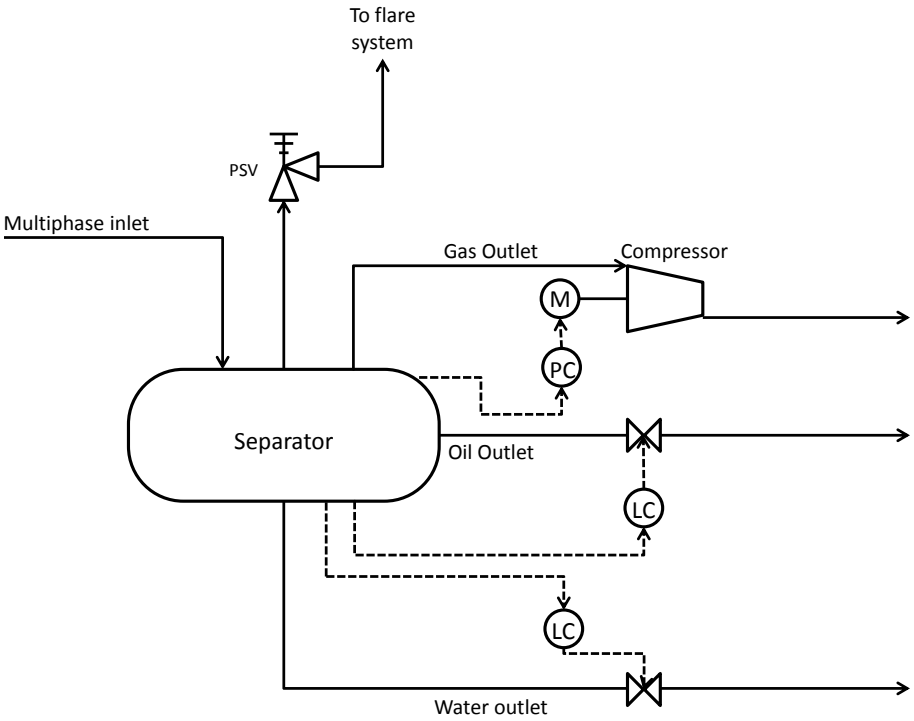

Figure 2.3: Schematic of a three-phase separator.

In order to export produced gas in an efficient manner, it needs to be compressed. The gas from the first stage separator (which is at high pressure) is compressed together with gas from the second and third separator (which has been compressed upstream), see figure 2.4. The inlet gas is cooled through heat exchangers and dried in scrubbers, which are liquid separating tanks, between each compressor stage.

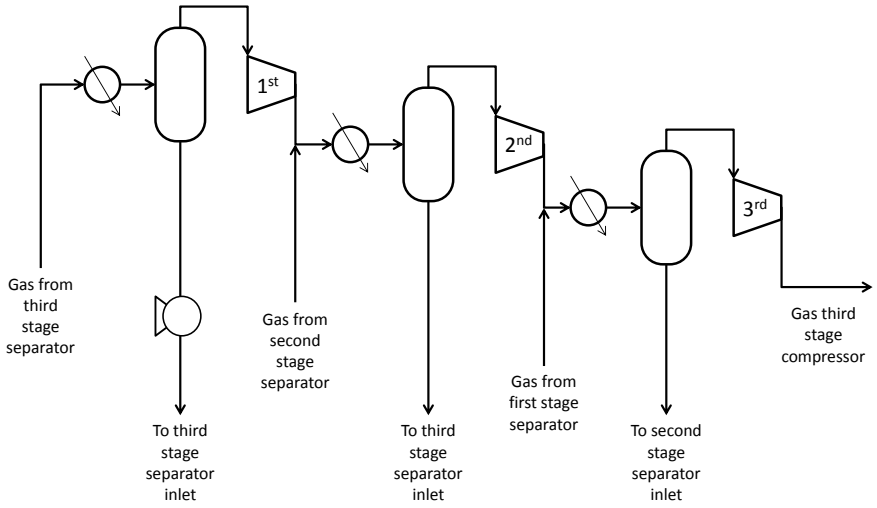

Figure 2.4: Compressor stages for compressing the gas. Every stage starts with cooling the ingoing gas and a scrubber for removing condensed liquid droplets. Separated liquid is sent back to the separators. [6]

2.3.2 Flare system

To avoid risk of open flame fire in the facility, controlled burning of the hydrocarbon gases is made by the flare system. Burning the hydrocarbons and chemicals in the flare and releasing carbon dioxide instead of hydrocarbons are less hazardous in a environmental point of view and less toxic than most hydrocarbons. Pressurised equipment handling hydrocarbons are connected to the flare system, resulting in an extensive piping across the production facility. All piping ends up in a vessel, called the knockout drum, where liquid that has been entrained with the gas can settle and be separated. The flare tip is often located on a structure, boom or tower outwards from the platform, directing the open flame away from the structure and the equipment. [12, 13]

2.4 Design of valves

Valves are used for controlling fluid flow in process industry. Several valve designs exist, which have different application areas. There are two main reasons why a valve needs to be installed: process control and process safety. Valves can be mounted for flow control, overpressure protection, back-flow prevention and fluid isolation. [14]

Ideally the flow velocity through a valve is proportional to the square root of the pressure drop. For specifying the flow/pressure relation one can calculate a flow coefficient [13, 15]. One of the more common ones are C_V, which is formulated as followed in equation 2.1:

$$C_V = \dot{V}\sqrt{\frac{G}{\Delta P}} \tag{2.1}$$

Where $\dot{V}$ is the volumetric flow through the valve in U.S. gal/min, G is the specific gravity of the fluid with water as reference fluid at 60°F and ΔP is the pressure difference over the valve in lb/in^2. The coefficient is valid for fully turbulent flow and newtonian fluids [14, 15]. C_V is one of the most used coefficient for determine the size of valves. When design choices of valves are made for non-newtonian fluids and multiphase flows, other correlations for calculating C_V exist. These are often provided by valve manufactures to give an equivalent C_V for their specific valves. [13, 14]

2.4.1 Valve characteristics

Depending on the valve function, the relation between valve C_V and valve opening is of importance. This relation is called valve characteristics or flow characteristics. The valve characteristic of a globe- or choke valve can be manipulated by changing the design of the trim cage or plug. There are three common valve characteristic groups; quick opening, linear and equal percentage. Usually, control valves are designed to have equal percentage characterisation. Equal percentage is characterised by a exponential increase of C_V, see figure 2.5. [15, 16]

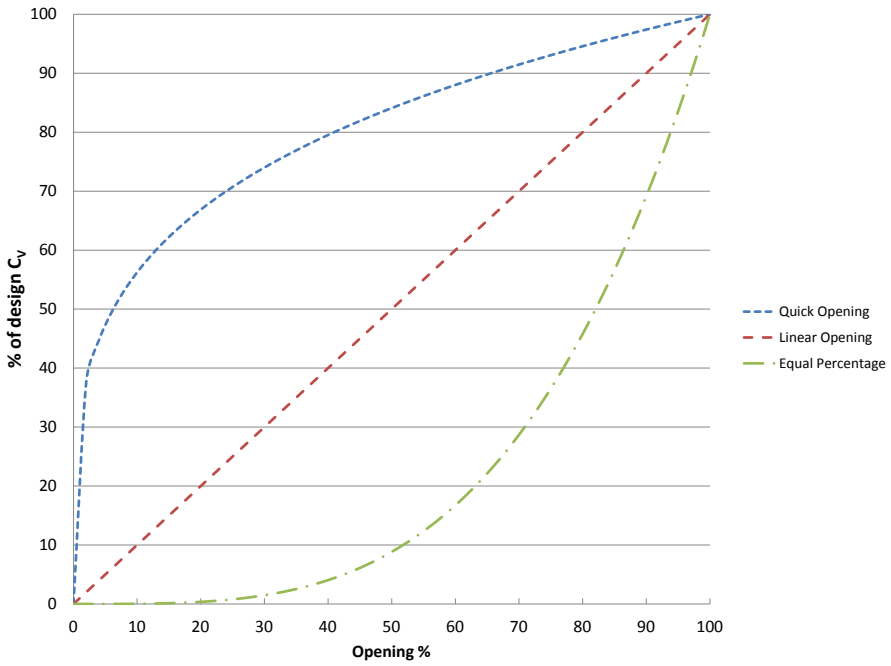

Figure 2.5: The three most common valve characteristics [15, 16].

2.4.2 Choke valves

A control valve for controlling the production rate in offshore industry is called a choke valve. Chokes are mainly operated by the process operator and are often situated both subsea at the wellhead and topside before the manifolds. [17]

2.4.3 Pressure safety valves

For protecting equipment from overpressure, pressure safety valves (PSV) can be mounted to release fluid to reduce pressure. PSVs are designed to open at a specific pressure, a set pressure, which is set to keep the affected equipment and piping below its pressure limit. In case of not harmful substances the relief valve can release directly to the atmosphere or in case of harmful substances to a sealed containment or a flare system. Pressure relief valves can be seen as an orifice which opens at a specific pressure. The mass flow through the valve is dependent upon the area of the orifice. [14, 15]

2.5 Flow assurance

Flow assurance is a field within oil and gas production engineering for securing continuous production of hydrocarbons [18, 19]. It consists in brief of fluid mechanics, heat transfer and chemical formations. Flow assurance is used to analyse phenomenons such as hydrate formation, waxing and determining of flow regimes (such as slugging), pressure drops, temperature changes and production rate [18, 19]. By analysing the pipeline flow it is possible to find an optimal design which can lead to a optimal balance between capital and operating costs [19].

2.5.1 Wax formation

Wax deposit is a severe issue in flowlines and pipelines. When crude oil is cooled the long alkane substances and paraffin waxes can form wax crystals and precipitate from the oil. These crystals can stick to the interior of the pipe, instruments and valves which can cause blockage and malfunction. If the wax deposits over a long period it can lead to total blockage of the pipe and production shut down. [19, 20]

To clean the interior of the pipe plugs, which are called pigs, are occasionally inserted at the inlet. As the pig is travelling with the flow it scrapes off deposits on the pipe wall reducing the build up. This operation is called pigging. [19, 20]

To prevent formation of wax deposits, pipe interior can be heated or insulated to decrease cooling of the fluid. Different chemical inhibitors can also be injected to inhibit the formation rate. [19, 20]

2.5.2 Hydrate formation

At high pressures and low temperatures water and hydrocarbons form crystals, called hydrates, where the water molecules encapsulate hydrocarbons forming an ice/snow-like substance. These crystals can, similar to waxes, block the flow and cause production stop and malfunctions. To prevent hydrate ice to form heating of fluid and injection of inhibitors, such as methanol and ethylene glycol, are usually introduced. [19, 21]

2.6 Multiphase flow in pipes

Dealing with single phase flow in pipes is quite straightforward. The complexity of single phase flow is bounded to one phase and its interaction with solid boundaries. In multiphase flow, the complexity increases dramatically. Each phase has its own flow behaviour and all phases interact through their interacting surfaces. The variability is endless due to the non-rigid interphases. This makes multiphase flow more difficult to numerically solve and model. [8, 22]

2.6.1 Flow regimes

In multiphase flow in pipes the categorization of different dispersions of the fluids are called flow regimes [8]. In general, the flow regime is due to the interaction between the phases. Some variables have greater effect on the flow regime such as the geometry of the pipe, velocity of the phases, viscosity, volume fraction of the phases and the surface tension. The flow regime in a pipe can have impact on equipment performance. Unstable and uneven flow can lead to instability in process control and to reduced performance and production. [8, 22]

In horizontally arranged pipes, flow regimes with greatly segregated phases will be significantly more dependent of gravity, see flow regime c-f in figure 2.6. If the pipe follows a hilly topography the densest phase will due to gravity accumulate in the segment between two peaks. When the lighter phase pushes the denser phase forward slug flow can be formed. This is called "terrain generated slugging". This is common for oil and gas subsea pipelines. [8]

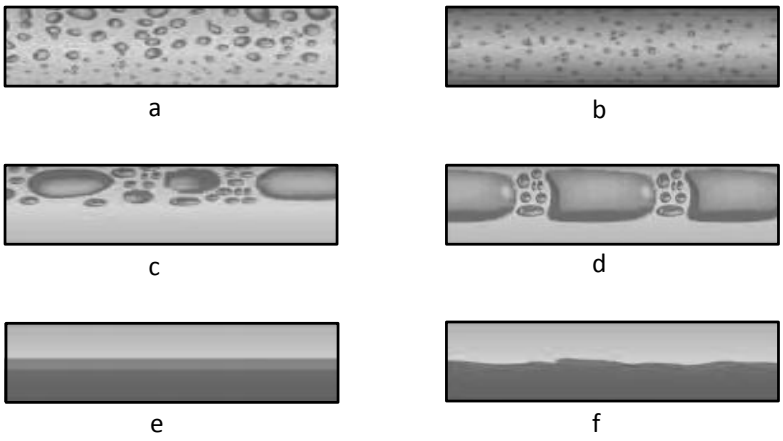

Figure 2.6: Some typical flow regimes for two phase flow in horizontal pipes. a: Dispersed bubble flow, b: Annular flow, c: Elongated bubble flow, d: Slug flow, e: Stratified flow, f: Stratified wavy flow. Re-created from [8].

For vertically arranged pipes gravity is symmetrically distributed over the cross-sectional area. This results in an averaged symmetrical distribution of the phases. This gives other specific flow regimes for vertical pipes, see figure 2.7. [8]

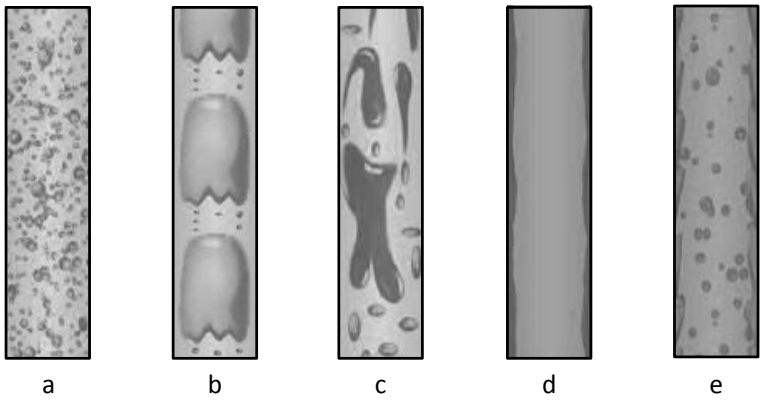

Figure 2.7: Some typical flow regimes for two phase flow in vertical pipes. a: Dispersed bubble flow, b: Slug flow, c: Churn flow, d: Annular flow, e: Annular flow with droplets. Re-created from [8]

In long oil and gas bore holes or pipelines where there is a significant pressure drop it is common that the flow regime changes along the pipe. As the pressure decreases dissolved gas and light components will vapourise, increasing the volume fraction of gas. When the flow regime results in a severe segregation of the phases, such as slug flow, downstream connected equipment and controllers can be affected. If for example slug flow occurs in a production riser the downstream separator unit will have periods with only gas flow and periods with only oil flow. To keep constant

liquid levels and pressure in the separator the controllers will need to regulate the flow constantly resulting in unstable production. [8, 22]

2.7 Modelling and simulation of industrial processes

Oil and gas well fluid often consists of three phases: oil, gas and water. A three phase flow has an increased complexity which also increases the number of possible flow regimes. This kind of system is often modeled by simplification through averaging the the liquid phases, and the system is modeled as a two phase system. Several models have been developed and implemented in process tools. [8]

Generally, a model has the purpose to predict a real system or process. The system to be modelled can be of a wide range of types and the model itself can be in a lot of different forms. Mathematical models are widely used in engineering applications. A mathematical model uses equations and variables to describe the behaviour of an event [23, 24]. Offshore production systems are a kind of industrial processes which often are evaluated using mathematical models. The real problem is transformed to a mathematical problem which generates a mathematical solution which subsequently can be interpreted [23]. A model is limited by the knowledge about the system to be modelled but a well defined model, where the correct equations and assumptions are used, can be a help to understand the process and predict behaviours in a sufficient way [24].

The definition of an industrial process is that it constitutes a production of a product with specific properties done by physical and/or chemical modifications during controlled conditions [24]. Design and construction of an industrial process plant requires a lot of information about the process which is to be carried out in the plant [23–25]. Use of mathematical models for decision making in the design phase reduces the risk of rapidly increased costs due to reconstruction of the process equipment in a late stage. A better understanding of the industrial process leads to improved process optimization, design and control. In addition, safety aspects and environmental aspects can be evaluated with more accurate results [26]. The continuous development of computational capacity contributes to improved modelling and keeps the modelling tools up-to-date. Hence, modelling and simulation are relevant procedures in building or redesigning plants and equipment for industrial processes. [23]

2.7.1 Historical background of modelling of industrial processes

During the industrial revolution, which began to take place in the late 18th century and continued through the 19th century, the process industry grew larger and the processes became more complex. The field of chemical engineering evolved and the

use of unit operations began to take place during this era [23, 27]. To solve the mass and energy balances for the unit operations, the use of mathematical modelling increased.

Modelling and simulation of chemical processes is a fundamental part of the larger concept called *process systems engineering*. Process systems engineering involves process design, optimization of system operations, mathematical modelling and simulation of the systems' behaviour. The studies of transport phenomena and calculations of conservation of mass, momentum and energy have been contributing to the development of mathematical modelling as well as the increasing computational capacity. [23, 27]

The first commercial simulation tool for chemical industries was created during the 1960s. This is still a great milestone in the historical technical development within the field of chemical engineering. By then, it was possible to make a quantitative evaluation of a chemical plant's operations. As computers with better performance developed continuously it was possible to make improved simulation software. By the year of 2011 there were six commercial modelling and simulation software programs available on the market. [27] When the PC was invented in the 1980s the use of simulation tools was enhanced and both steady state and dynamic simulations could be used among process engineers in the industry [23].

During the start of the 21st century the tools for modelling and simulation have continued to be improved and still continues to be improved. Stephanopoulos [27] argues that one of the areas within process systems engineering to be developed further in the future is to enhance the numerical methods for more complicated systems. Probably, it will in the future be possible to simulate systems that are even more complex and containing a larger span between the boundaries of the system than what is possible today.

2.7.2 Modelling of oil and gas production processes

As mentioned in section 2.6 the fluid from the reservoir contains a mixture of mainly hydrocarbons and water with high pressure and temperature. Thus, mathematical models are required to describe the physical properties of the flow accurately. To yield the physical properties of a mixture correlations of pressure, volume and temperature (PVT) should be established in a model. One method to establish PVT correlations is to use so called *equations of state* (EOS) [14].

2.7.2.1 Equations of state

An equation of state is an equation which describes how the molar volume of a real gas and liquid depends on pressure and temperature [13]. The simplest and most basic equation of state is the ideal gas law [28]. A gas can be considered ideal at pressures below 4 bar, hence the gas is non-ideal if the pressure is higher and the ideal

gas law can no longer be considered as valid. Several different forms of equations of state have been developed and all of them contains at least one empirical constant [14].

The van der Waals EOS was the first to describe a mixture with both liquid and vapor phases. This EOS is not used in industrial models, though several modified EOS' with origin in the van der Waals EOS have been developed and implemented in industrial simulators [14]. The van der Waals EOS was the first equation of state in cubic form [29] and since the early 1980s the cubic equations of states have become successful in describing physical properties of mixtures of hydrocarbons [14]. Non-cubic EOS have been proven not to give the same accuracy in the results as from the cubic equations when modelling large reservoirs [29].

One of the most common equations of state used in modelling of oil and gas processes in pipelines is the Peng-Robinson EOS:

$$P = \frac{RT}{\nu - b} - \frac{a(T)}{\nu(\nu + b) + b(\nu - b)} \tag{2.2}$$

where ν is the molar volume and a and b are empirical correlation constants. Equation 2.2 is developed from the van der Waals EOS and the major benefit from using the Peng-Robinson EOS is the improved prediction of liquid phase densities [30].

2.7.2.2 Hypothetical components

When modelling the production of crude oil and gas, physical properties such as critical temperature and critical pressure of the components need to be specified [19]. The number of hydrocarbon compounds in a reservoir mixture can be over one million and it is not possible to model such large number of components separately [9, 13]. Heavier components are instead lumped together and the boiling point is set from a mean value of the lumped components' boiling points. Generally, components with seven carbon atoms or more are lumped together [19]. These lumped components are called hypothetical components or pseudo components. The properties of the mixtures in different wells are unequal, hence specifying special hypothetical components for the reservoir of interest leads to the best prediction of the behaviour of the flow. Commercial simulators have pre-formulated hypothetical components and it is also possible to add an own list of hypothetical components [13]. It is recommended to use four to ten hypothetical components during simulations to receive an acceptable result [31].

2.7.2.3 Pressure-drop correlation models

Modelling of oil and gas production processes requires estimations of the pressure drop and liquid holdup in pipes. There are several models proposed for pressure

correlations in multiphase flows. Many of these models are established for either horizontal or vertical flow and are not as accurate for inclined flow [32, 33]. The pipelines in offshore oil and gas production stretches up to several kilometers over the seabed which often can have a hilly terrain. Thus, it is necessary to have models suitable for inclined pipe flow as well [33].

H. Dale Beggs and James P. Brill [32] were two of the first to conduct models with better pressure drop predictions for inclined flow. They discovered the weakness in the existing pressure correlations when predicting the pressure drop in wells drilled in an angle with high deviation from vertical. If the pipe flow would contain only one phase the pressure drop in the uphill flow is recovered in the downhill flow. Though, in multiphase flows, the liquid holdup is lower in the downhill flow compared to in the uphill flow. This should be taken into account when modelling pipelines with a mixture of oil, gas and water [32].

Beggs and Brill discovered that the pipe inclination has a definite effect on the liquid holdup and pressure drop for flows in inclined pipes. When calculating the pressure gradient in a pipe there are two unknowns: the liquid holdup and the friction factor. Beggs and Brill proposed a model with improved correlations for estimating the liquid hold up and the friction factor in inclined pipes [32]. The Beggs and Brill pressure-drop correlation proves to accurately predict the holdup in uphill flow, though it overpredicts the liquid holdup in downhill flow. Due to the overprediction of liquid holdup in downhill flow the model underpredicts the pressure losses in these cases. [33]

For vertical multiphase flows, Duns and Ros [34] have developed a pressure drop correlation model improved for different types of flows and for mixtures with varying compositions. The model contains separate correlations for liquid holdup and friction losses for a number of different flow regimes: bubble flow, plug flow, froth flow, slug flow and mist flow [34, 35].

HTFS is a proprietary pressure drop correlation model developed by Aspen HTFS Research Network in the Aspen Tech company [36]. To calculate the frictional pressure drop, the pressure drop for each separate phase is calculated first. The frictional pressure drop calculation is then based on a correlation between the pressure drop calculations for the phases together with a correction factor. The model is suitable for horizontal, upward inclination and downward inclination. [35]

The pressure drop correlations predict the flow regime and use correlations specified for the predicted flow regime to calculate the pressure loss. In HYSYS, if there are two liquid phases present, one single pseudo liquid phase is calculated by using empirical mixing rules. [35]

2.7.3 Dynamic simulations of oil and gas production systems

When a process is stable and produces at a constant rate the time dependency is negligible, hence the process is at steady state conditions. A process in steady state is therefore modelled without a time variable [24]. In contrast, a dynamic model solves the conservation equations in each time step [37].

Steady state simulations require less computational time and capacity than dynamic simulations and are sufficient for cases where the flow is not varying over time [37]. For larger segments, for example kilometre-long pipelines, the unsteady nature of the flow will result in a transient behaviour. Hence, dynamic simulations are adequate for a reliable prediction of the system [38]. If a sudden change in the system occurs dynamic simulations are required to study the behaviour of the process during this change [39].

Generally, when designing offshore production systems, the different units such as (for example) the flowline and the separator are modelled and designed separately. For the facility to be operated safely the units will be designed to endure conservative scenarios. Though, an overestimation of the size and weight might be made and can, in the worst case, lead to an unfeasible design choice. Dynamic simulation software use programmed rigorous models and will give a better prediction of the transient flow behaviour. Dynamic simulation is also useful when studying start-up and shut-down procedures as well as extreme cases such as an unintended opening of a choke. The dynamic simulation can be used to evaluate and improve the control philosophy of the production process. [39]

3 Methodology

In order to conduct simulations which represents a real scenario an existing satellite field's flowline, riser and relevant topside equipment are chosen as basis. This chapter describes the model used in the simulations and all the included segments and units. Specifications of the three-phase fluid are also formulated. The model was validated through comparisons with production data from the satellite field and for three different production dates. This chapter also contains description of the simulated scenarios: production start-up, shut-down and choke collapse.

3.1 Model formulation

A steady state model was first built to resemble steady production data, which was used as an initialisation for the dynamic simulations. To perform this, relevant system specifications are known for the chosen field and simulations were performed to validate the model. Chemical composition and properties of the streams are also known. The Aspen HYSYS Hydraulics model was used due to the more rigorous calculations and connection between segments [40]. A schematic of the complete model is shown in Appendix A and the sub-flowsheets will be described in further detail in the following sections. The ambient temperature of the water surrounding the subsea equipment is set to 5 °C. The EOS Peng-Robinson was chosen due to it's well-established advantages for prediction of characteristics for gas and oil flows.

3.1.1 Well trajectory

The flow inlet is located at the well inlet adjacent to the reservoir. The production reservoir is located vertically 1820 meters below and 1100 meters horizontally from the wellhead. The well is drilled in a curve from the reservoir to the wellhead choke, located 250 meters below the sea surface. A sketch of the model used in the simulations is shown in figure 3.1. The main reason the well is included in the model is to consider the volume of the well when studying the behaviour of the flow during different dynamic scenarios. Due to this, the well is modelled as a standard pipe segment in Aspen HYSYS. The well route is simplified to consist of 14 segments,

with narrower segments in the bend of the curve where the direction of the pipe changes from vertical to horizontal.

The inner diameter of the well pipe is 6 inches and the roughness of the pipe material is set to $1{\cdot}10^{-4}$ meters. The ambient temperature is 5°C and an overall heat transfer coefficient for the pipe is set to 5.1 $W/(m^2K)$. The settings used in the model are based on standardised values for wells.

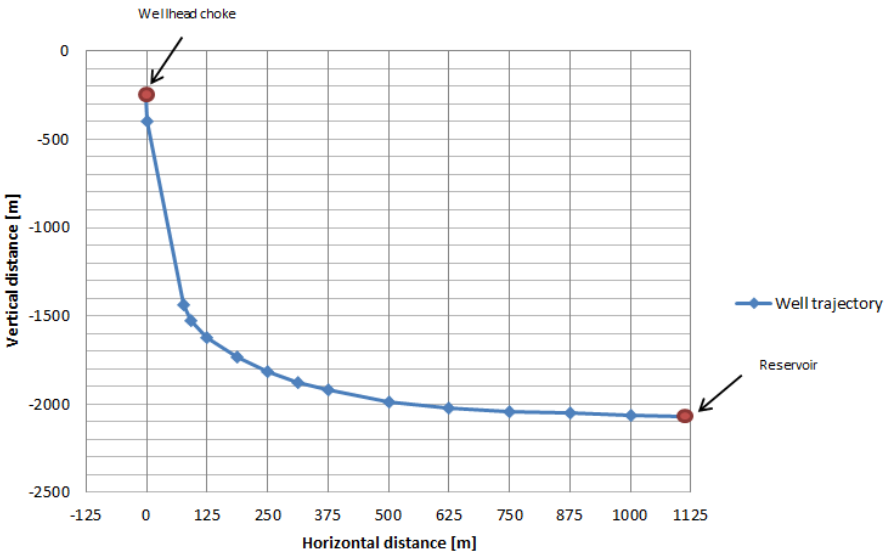

Figure 3.1: Well trajectory from the reservoir up to the wellhead choke located at a water depth of 250 m. The markers show the distance between the segments in the model.

3.1.2 Flowline specification

In order to formulate an accurate model of the flowline and riser the routing of the pipeline on the seabed was available through mapping of the seabed. The horizontal distance on the seabed is 20 kilometers at a depth between 260 and 335 meters. The flowline is downwardly sloping from the wellhead towards the production platform, shown in figure 3.2. The routing of the flowline was for the model coarsened to consist of 33 equally long segments with an elevation change corresponding to that of the pipe route, see figure 3.3. Each segment is 625 m long and is divided into 10 computational cells.

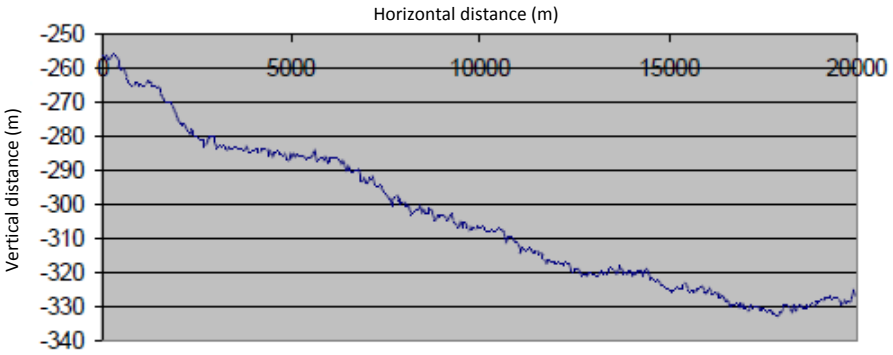

Figure 3.2: Routing of the flowline along the seabed from the wellhead to the riser base.

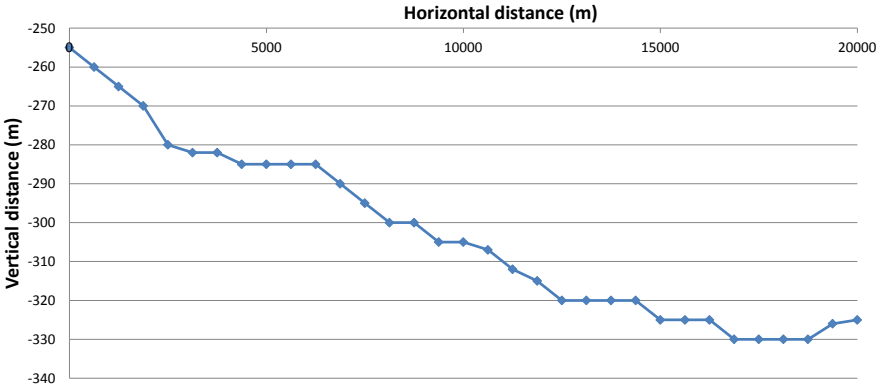

Figure 3.3: Routing of the flowline used in the model.

The flowline stretches from the wellhead choke to the riser base. In the real system, the stream goes through some piping in the well template, see section 2.2.3. The pressure drop from the template is not included in the model. The inner diameter of the flowline is 9 inches and with a roughness of $5 \cdot 10^{-5}$ meters. The overall heat transfer coefficient is estimated for the flowline to be around 1 W/(m^{2}K). However, the thickness of the insulation material was adjusted to fit with temperature data from the cases. The flowline is modelled using Aspen Hydraulics pipe segment. The HTFS pressure-drop correlation model was applied in the flowline. This was chosen due to its applicability for horizontal and downward inclination flows. It was also chosen based on experience from a pre-study evaluation of pressure drop correlations in the flowline and the riser, these evaluations are not described further in the thesis.

3.1.3 Riser specification

The riser length and sea depth were known, but not the elevation profile from the template to the platform. The riser was therefore constructed out of three segments with different elevations, see figure 3.4. It was known that the riser had a S-shape and was chosen to be incorporated in the model. The diameter of the riser is 7

inch and the wall roughness is $7 \cdot 10^{-4}$ meters. The overall heat transfer coefficient is set to 10 W/(m^{2}K). The riser was modelled in Aspen Hydraulics pipe segment. As for the riser, the pressure drop correlations were chosen by the same reason as for the flowline; by testing different pressure drop correlations and comparing with existing data. The upward inclination from the riserbase to the bend and the downward inclination are using the Beggs and Brill (1979) [33] pressure drop correlation method. Since the Beggs and Brill method predicts vertical flow less accurately, the Duns and Ros pressure drop correlation was implemented in the last segment which is almost vertical. The Duns and Ros model is specified to predict vertical flows.

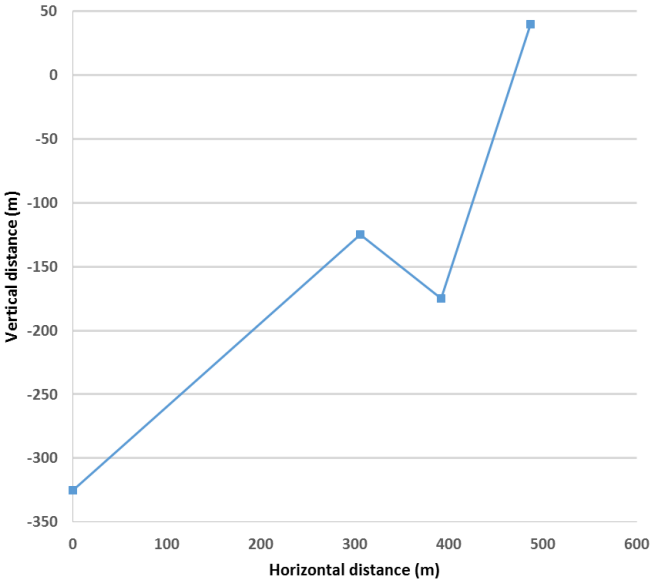

Figure 3.4: Riser elevation used in the model.

3.1.4 Separator unit

For the dynamic choke collapse scenarios the separation process was included in the model and its flow sheet is shown in figure 3.5. Upstream the three-phase separator the production flow is collected in a manifold together with the production from additional wells tied to the same platform. In the simulated scenarios the production is led towards the second stage separator, operating at 20 bar.

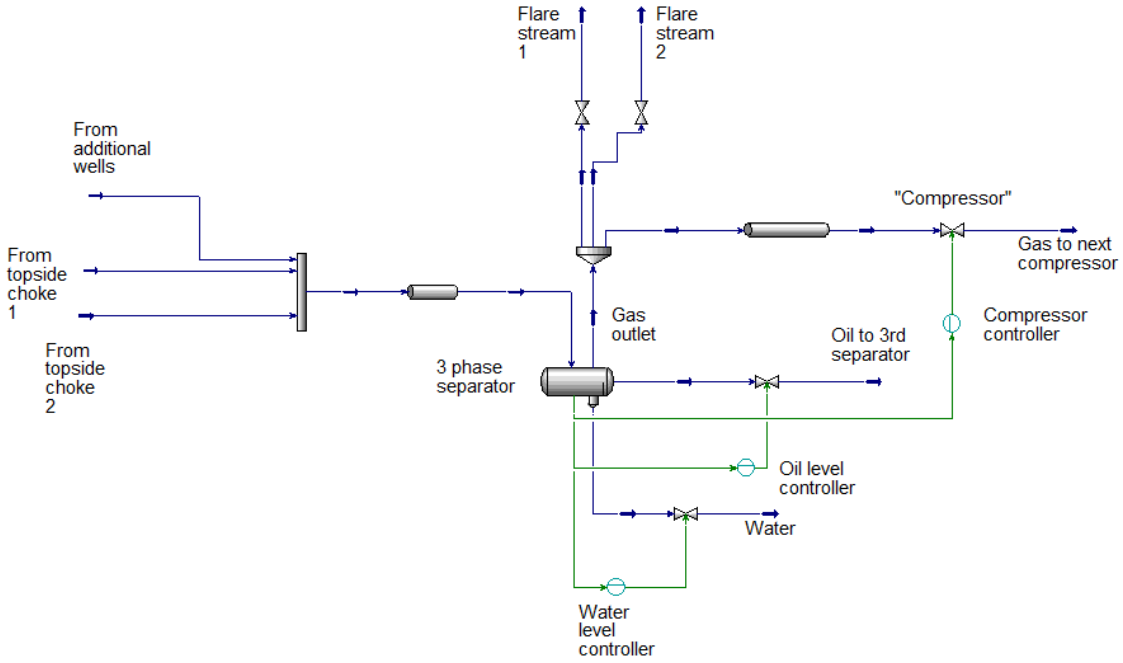

Figure 3.5: The process flow sheet of the separation used in the simulations.

To simplify the model, the compressor which is compressing the gas from the separator is modelled as a valve. The motor driving the compressor is set to be working at maximum power. If the maximum capacity of the motor is reached it will shut down to avoid overheating, also known as tripping. In the model, the "compressor valve" opening is regulated to keep the pressure in the separator at 20 bar. The outlet pressure is set to atmospheric pressure. The maximum volume capacity when the motor is running at full power is used to calculate a C_V for the "compressor valve". Hence, the tripping of the motor is simulated by using a cause and effect matrix to close the valve after the valve reaches 100% opening. When the cause and effect matrix is activated the actuator will close the valve linearly during 10 seconds, simulating a realistic compressor shut-down.

As mentioned earlier, the process model is based on an existing platform. The modelled platform has two pressure relief valves connected to the second stage separator. The relief valves have a set pressure of 40 bar and a full open pressure of 44 bar. It is also known that the separator has a rupture disc installed which ruptures at a pressure of 45.7 bar. However, these are not included in the model. The oil level and water level in the separator are maintained by control valves at each outlet.

3.1.5 Flare system

A simplified model of the flare system was included in the topside model. The main reason was to include the volume in the flare system to evaluate its dynamic effect. Due to this, possible increments in the piping have not been considered in the model and the piping is modelled with pipe segments in Aspen HYSYS. Figure 3.6 shows

the model of the flare system used in the simulations. In reality, the flare system consists of extensive piping from other process units at the production facility. The volume of the piping which is not directly linking the second stage separator to the flare tip is summed up and added to the knockout drum. The total volume of the piping and knockout drum in the flare system is 161 m^3. The orifice of the flare tip is modelled as a valve.

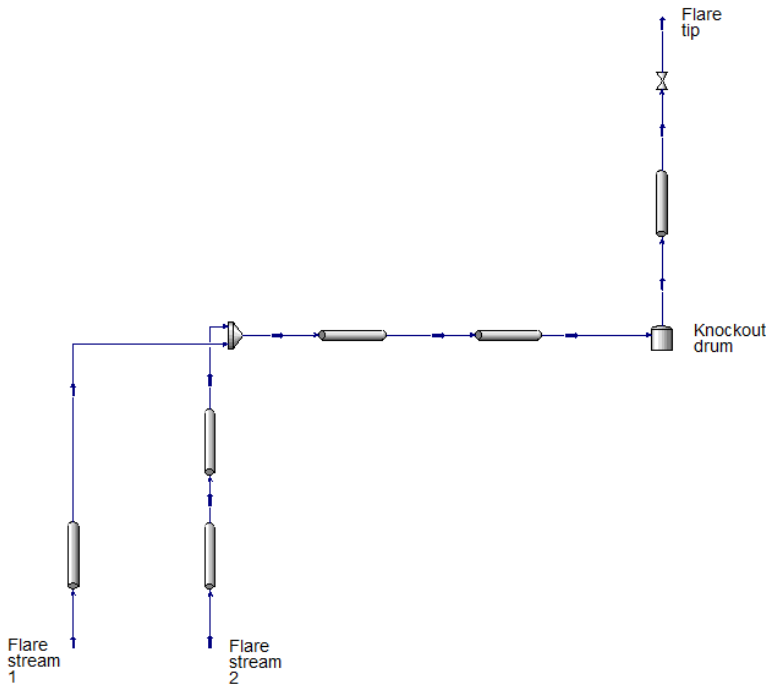

Figure 3.6: The flare system modelled in Aspen HYSYS.

3.1.6 Valve design and characteristics

In order to correctly evaluate flow through valves valve characteristic and C_V were determined from equipment design data. In Aspen HYSYS some valve manufacturer specific sizing methods are pre-programmed.

Regarding sizing of multiphase flow valves, manufacturer specified methods were used in the equipment specifications. For the topside chokes the manufacturer method was not available in Aspen HYSYS. Instead the default method in HYSYS (ANSI/ISA standard [41]) was used. Data of composition, flow and pressure drop were extracted from operational cases with different valve openings. A design C_V was then calculated for each case. From this, a valve characteristic curve could be extracted and it is shown in figure 3.7.

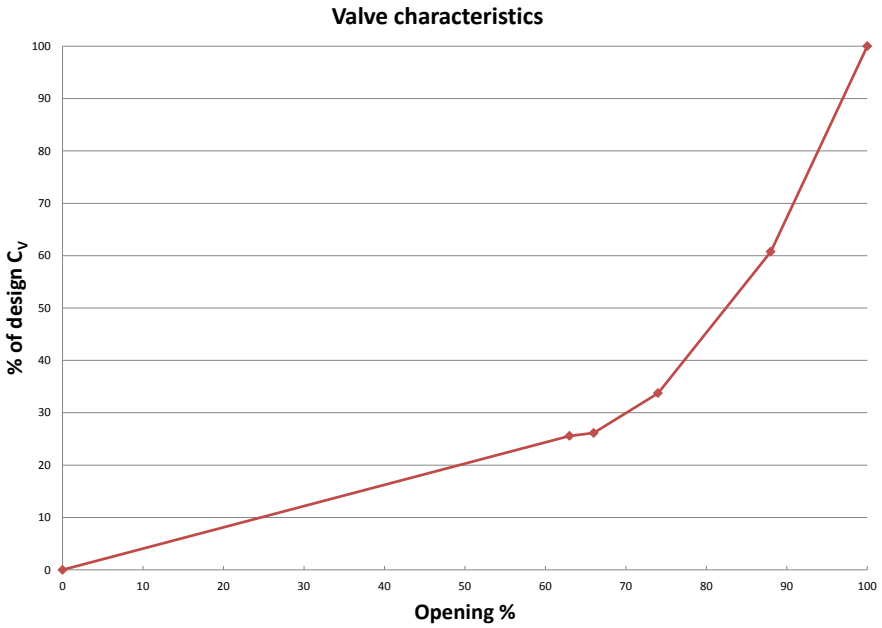

Figure 3.7: Valve characteristic curve generated using the ANSI/ISA method.

The curve was validated through hand calculation of the manufacturer's C_V method. The estimated curve in the figure has similar characteristics as an equal percentage curve, with an exponential increase in C_V when the valve opening increases. The curve in figure 3.7 is a rough estimation due to that the valve only operates at a few different values for the valve opening. The curve was implemented in the topside chokes' models.

3.2 Formulation of reservoir fluid

To be able to validate the model properly against the production data the fluid characteristics were specified. Chemical specifications from lab analysis of the existing reservoir were given as well as the gas-to-oil ratio, GOR.

3.2.1 Chemical specifications

Chemical components of the well stream are known through lab analysis. Heavier components than n-Hexane were defined as pseudo components, in HYSYS known as hypothetical components. Properties of lighter components were taken from the Aspen HYSYS property package library. To reduce the number of components in the model a large number of chemical species were lumped into hypothetical components which represent a range of species, see table 3.1. The properties of the hypothetical components were obtained by data from experimental results of the reservoir fluid.

Table 3.1: Chemical components in the system. Note that there are two tables next to each other.

Component	Properties
H2O	Known
Nitrogen	Known
CO2	Known
H2S	Known
Methane	Known
Ethane	Known
Propane	Known
i-Butane	Known
n-Butane	Known
i-Pentane	Known
n-Pentane	Known
n-Hexane	Known

Component	Properties
C_7	Experimentally determined
C_8	Experimentally determined
C_9	Experimentally determined
$C_{10}-C_{11}$	Experimentally determined
$C_{12}-C_{13}$	Experimentally determined
$C_{14}-C_{15}$	Experimentally determined
$C_{16}-C_{17}$	Experimentally determined
$C_{18}-C_{19}$	Experimentally determined
$C_{20}-C_{23}$	Experimentally determined
$C_{24}-C_{28}$	Experimentally determined
$C_{29}-C_{36}$	Experimentally determined
$C_{37}-C_{80}$	Experimentally determined

3.2.2 Determine and adjusting GOR and watercut

To determine the GOR in the simulations a system of three serial connected flashes with a set pressure drop and temperature was used. The construction of the GOR calculator is based on the same principles that are used in the multiphase meters located at the production facility. The flowsheet is shown in figure 3.8.

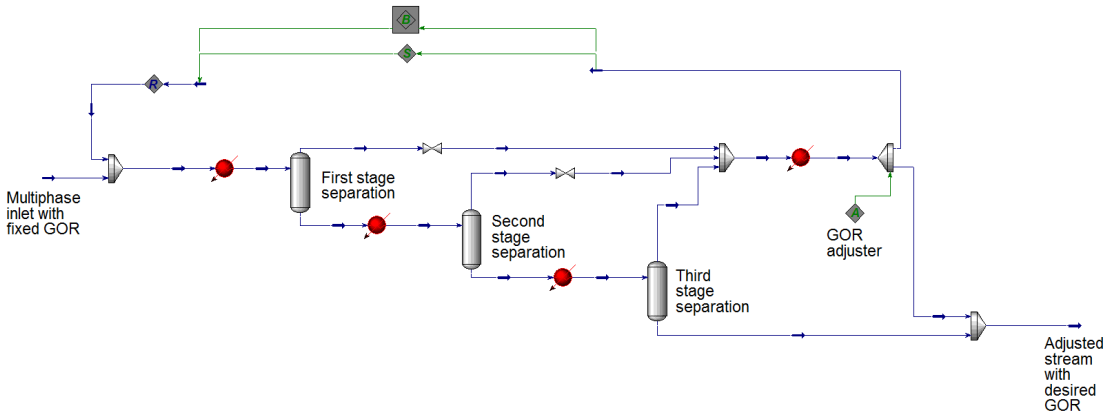

Figure 3.8: Schematics of the three stage separation used to determine and adjusting the GOR.

The first separator operates at 65 °C and 70 bar, the second separator at 60 °C and 20 bar and the last separator is set to standard conditions (15 °C and 1 atm). To start simulations with the given reservoir conditions, the GOR can be adjusted by recycling a part of the gas in the outlet stream into the inlet stream, as shown in 3.8. The existing well, which the model is based on, has gas lift for production cases when the water cut is high. The gas is injected into the well at approximately 1500

meters below the wellhead choke. The GOR obtained from the production data is the total GOR from the well, including the gas lift. The gas lift is thus included in the GOR adjustment.

The water cut in the reservoir will vary over the lifetime of the reservoir. Thus, the amount of water is adjusted in every simulation case by adding the correct water volume flow after the GOR is adjusted.

3.3 Model validation

To evaluate the pressure drop and temperature drop in the flowline and the riser steady state simulations were performed and validated with existing production data. The model used in the validation simulations included the subsea choke, flowline and the riser. Three production cases (I, II and III) with different boundary conditions were used, stated in table 3.2. The existing subsea system of choice contains two multiphase flow meters: one at the wellhead and two upstream the topside chokes. The multiphase flow meters measure production rates of oil, gas and water. The topside multiphase flow meter is the primary fiscal meter and calibrated against the test separator regularly. Hence, production data from the topside multiphase meter was used for the model validation. The subsea multiphase meter serves as a backup if one or both of the topside meters would be out of order. Deviations in hydrocarbon mass flow rate between the subsea meter and the topside meters are logged and if the deviations become larger than the set point, a warning signal is generated.

Table 3.2: Boundary conditions for the model validation.

	Wellhead pressure [bar]	Upstream topside choke pressure [bar]	Wellhead temperature [°C]	GOR	Watercut
I	93.9	66.2	73.0	381	0.13
II	71.4	32.8	80.5	234	0.35
III	65.4	19.2	79.1	301	0.48

Data for the three cases stated in table 3.2 are taken from production data from the chosen existing satellite field. The values are averaged values of measurements every fifth minute during 12 hours. The valve opening in the topside chokes are also taken from the existing production data for each production case. It is seven months between case I and case II and five months between case II and case III.

3.4 Simulation scenarios

Three dynamic scenarios have been conducted; shut-down of production; start-up of production and choke collapse. The shut-down and start-up scenarios were compared with operational data. The choke collapse scenario was simulated for four different configurations of the model.

3.4.1 Shut-down scenario

The boundary conditions for the shut-down scenario simulations are shown in table 3.3 and were set from operational data from a shut-down case. The model used in this simulation contains the well, flowline and riser.

Table 3.3: Boundary conditions for the shut-down and start-up scenarios.

Reservoir pressure [bar]	Downstream topside choke pressure [bar]	Reservoir temperature [°C]	GOR	Watercut
180.0	62.0	80.0	344	0.03

Opening percentage over time for the shut-down procedure was taken from operational data for the subsea choke and the topside chokes, see figure 3.9.

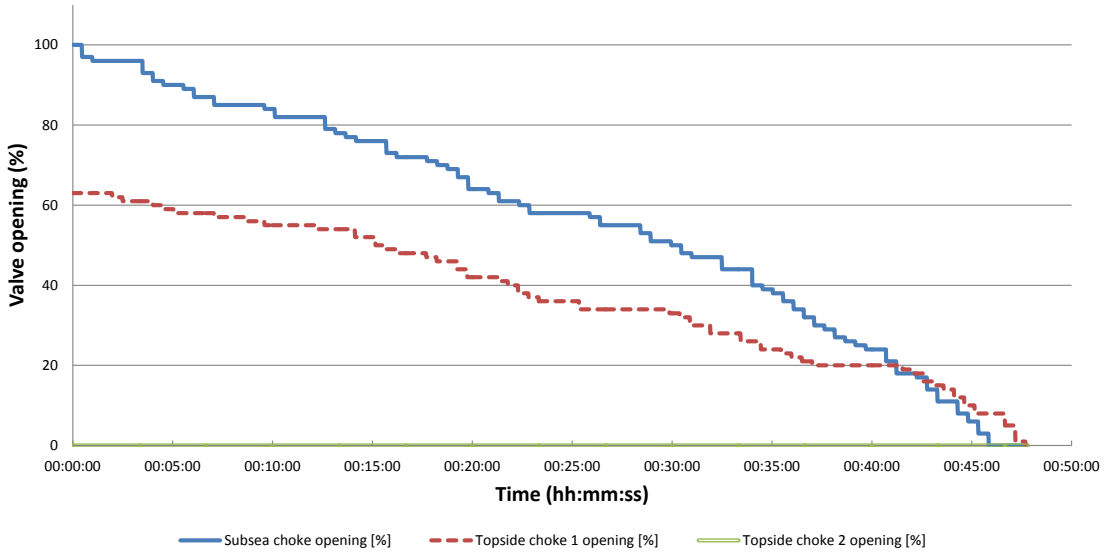

Figure 3.9: Shut-down sequence. The subsea choke is 100% open from the start. Topside choke 1 is 66% open and topside choke 2 is closed during the scenario.

The graph is simplified from the production data, the smallest changes in the shut-down procedure are lumped together. One of the topside chokes is closed during the whole scenario. As seen in figure 3.9, all of the valves are fully closed after

48 minutes. The procedure was inserted into Aspen HYSYS using the tool "Event sheduler".

3.4.2 Start-up scenario

The start-up scenario is based on data six days after the shut-down scenario data. The boundary conditions for the simulations are the same as for the shut-down case (table 3.3). The start-up procedure of the valves is shown in figure 3.10. As for the shut-down scenario, the valve opening data is taken from operational data. During this scenario topside choke 2 is not opened at all.

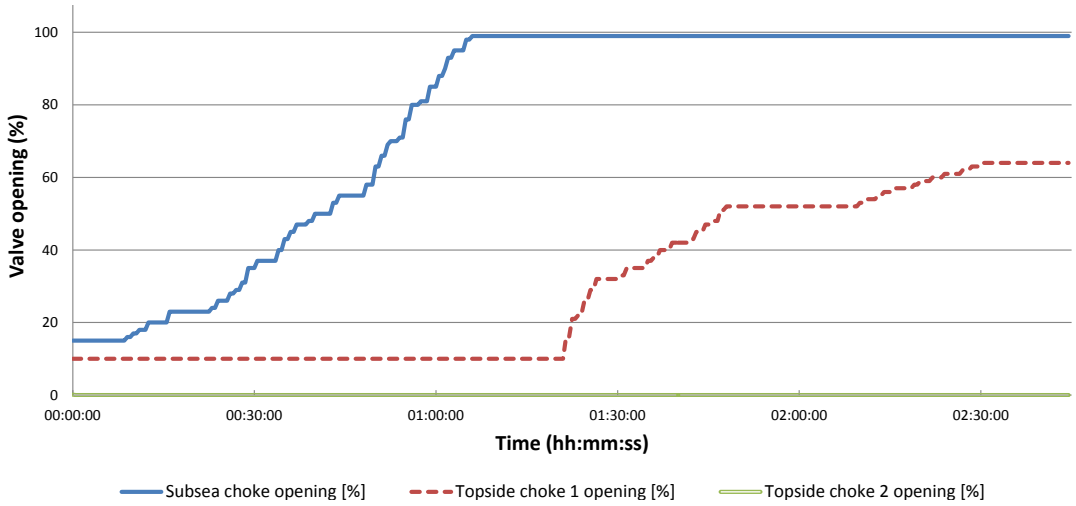

Figure 3.10: Start-up sequence. The subsea choke starts at 15% opening, topside choke 1 starts at 10% opening and topside choke 2 is closed during the whole event.

As seen in the graph (figure 3.10), the chokes are not completely closed from the start of the scenario, which is true for the real operational data. This is due to stability issues in the simulation software when the flow is low. The subsea choke is opened to 99% and topside choke 1 is opened to 64%. It takes approximately 2 h 20 min for the scenario to be completed.

3.4.3 Choke collapse scenario

For the choke collapse scenario several cases have been simulated with different levels of model complexity.

A choke collapse scenario, where the PSVs will open and release to the flare system, was formulated. The scenario starts with constant production with one topside choke fully closed and the other one 30% open which will build up a pressure difference between upstream the topside choke and the separator. To imitate a scenario where one choke collapses, both of the topside chokes are instantaneously opened to 100%.

Often, a choke collapse leads to a doubled flow capacity, hence both valves are opened suddenly in the simulations.

Four simulation cases have been formulated for the choke collapse scenario. The extension of the model for each case is shown in table 3.4.

Table 3.4: Simulation cases with different parts of the model included. The units marked with X are included in the specific cases.

Simulation case	Well (2538 m)	Flowline (20 000 m)	Riser (700 m)	Separator and flare system
A	X	X	X	X
B		X	X	X
C			X	X
D				X

The boundary conditions for the simulation cases are shown in table 3.5. The values for the inlet pressure and inlet temperature are taken from a steady state solution for the complete model (case A).

Table 3.5: Boundary conditions for the choke collapse scenario for the four different simulation cases.

Simulation case	Inlet	Inlet pressure [bar]	Inlet temperature [°C]	Separator pressure [bar]	GOR	Watercut
A	Reservoir	180.0	80.0	20.0	344	0.03
B	Upstream subsea choke	95.6	70.5	20.0	344	0.03
C	Upstream SSIV	84.3	58.8	20.0	344	0.03
D	Upstream topside choke	70.3	54.9	20.0	344	0.03

The flow from the topside chokes is collected in a manifold where production from other wells also is collected before the separator stage. The production from other wells are based on actual data from the existing platform and was set to 111 500 kg/h. Results of mass flow and pressures were extracted from relevant streams.

4 Results

Results from the model validation and the simulation scenarios are presented in this chapter. The shut-down scenario and the start-up scenario are compared with production data from the existing system, while the choke collapse scenario is not compared with any existing data.

4.1 Model validation

As described in section 3.3, the model was validated with operational data from an existing well. To achieve a thorough validation, three production dates, called I, II and III, were chosen for the validation. The comparison was made by different parameters, such as pressure, temperature, flow rate, GOR and watercut. For each of the cases, the simulation was run until it reached approximately 1000 simulated minutes and all of the cases were considered to have reached a steady state condition due to constant pressure, mass flow, temperature, GOR and watercut over time.

The results from the validation of oil volume flow and the riser base pressure are shown in table 4.1 and 4.2. Additional results for the model validation are shown in tables B.1-B.4 in Appendix B. All of the data have been used to validate the model. The column "Actual" contains values extracted from the operational data and the column "Model" contains the result from the simulations. The difference between the actual value and the model value is shown in the table as well as the percental difference between the values.

Table 4.1: Validation result of oil flow measured in standard cubic meters per day.

	Oil flow (Sm^3/d)			
	Actual	Model	Diff	Diff (%)
I	2 368.5	2 425.0	56.5	2.4
II	2 347.2	2 385.0	37.8	1.6
III	1 853.3	2 103.0	249.7	13.5

Table 4.1 shows that the difference from the actual value of the oil flow to the simulated flow is 2.4 % and 1.6 % for case I and II respectively. The difference is

almost 14% for case III.

Table 4.2: Validation result of the riser base pressure in bar.

	Riser base pressure (bar)			
	Actual	Model	Diff	Diff (%)
I	81.7	80.7	-1.0	-1.2
II	51.8	50.7	-1.1	-2.2
III	41.9	41.4	-0.5	-1.3

Table 4.2 shows that the deviations between the model and the value from the real production cases have a maximum deviation of up to 1.1 bar, or up to 2.2%. The results for GOR and Watercut (table B.2 and B.3) are shown in appendix B and are used to verify that the simulations were steady when the validation was made. When studying the tables B.1 and B.4 it is notable that for two of the cases, I and II, the temperature upstream the topside chokes is higher than the temperature at the riserbase.

4.2 Shut-down scenario

Results from the shut-down scenario are presented in this section (figure 4.1-4.4). Results from the simulations are compared with the operational data from a shut-down scenario.

Figure 4.1 and 4.2 show the pressure at different locations in the system together with the valve opening for the subsea choke and one of the topside chokes for both operational data and for simulation data. The second topside choke is closed during this scenario. The locations from where the pressure data is taken from are: the wellhead, downstream wellhead, upstream riserbase and upstream topside chokes. During simulation of the shut-down scenario a stability issue was detected when both chokes were fully closed, which resulted in that the solver did not converge and stopped. It is seen in the operational data, figure 4.1, that the pressure downstream the subsea choke is relatively constant during the shut-down, while the pressure upstream the choke increases to reach a pressure of 100.6 bar when fully closed. Pressure at the riserbase increases from 84.5 bar to 88.3 bar. Overall it is seen that the pressure decreases along the declining flowline.

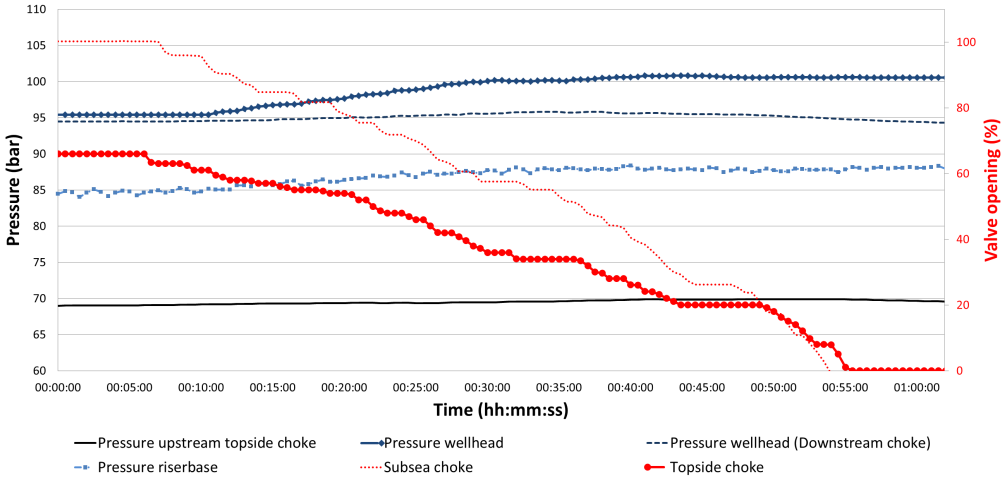

Figure 4.1: Recorded pressure over time during production shut-down for the facility. The pressure is seen at the left vertical axis and the valve opening percentage is seen at the right vertical axis.

For the simulation case, seen in figure 4.2, the wellhead pressure increases during a major period of the shut-down scenario until it eventually decreases. In the end, the shut-down results in an increase of the pressure upstream the subsea choke relative to before the closure. It is also seen that the pressure downstream the subsea choke (inlet of the flowline) and at the riserbase decreases during the shut-down. When both valves are completely closed the pressure is lower, 78.8 bar, at the inlet of the flowline than at the riserbase, where it is 79.5 bar. The pressure upstream the topside choke also decreases to 65.4 bar.

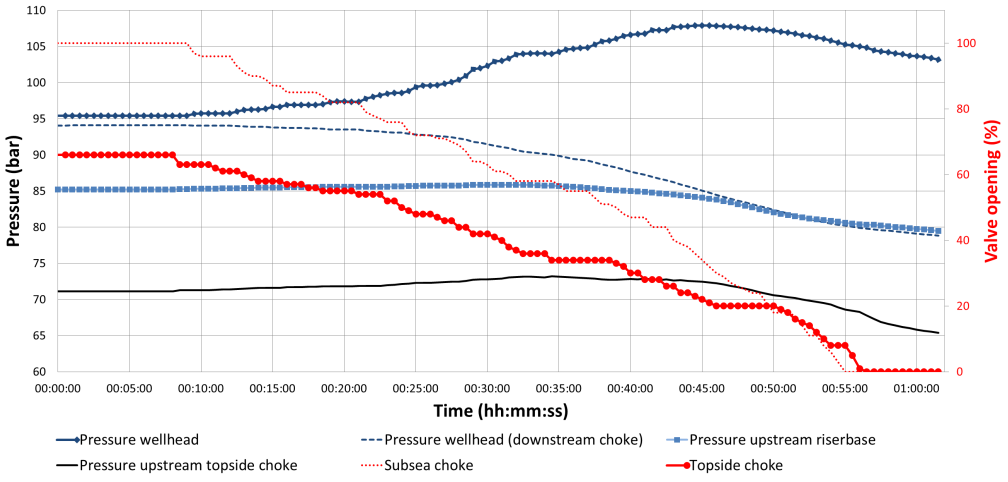

Figure 4.2: Pressure over time for the simulated shut-down. The pressure is seen at the left vertical axis and the valve opening percentage is seen at the right vertical axis.

The recorded data for the total mass flow and the total mass flow result from the simulation are shown in figure 4.3 and 4.4 respectively. In figure 4.3 it is seen that the mass flow fluctuates. During the shut-down sequence these fluctuations decreases in the later stage of the sequence. A flow reading is also seen when both valves are closed. However, this is assumed to be a misreading by the multiphase meter.

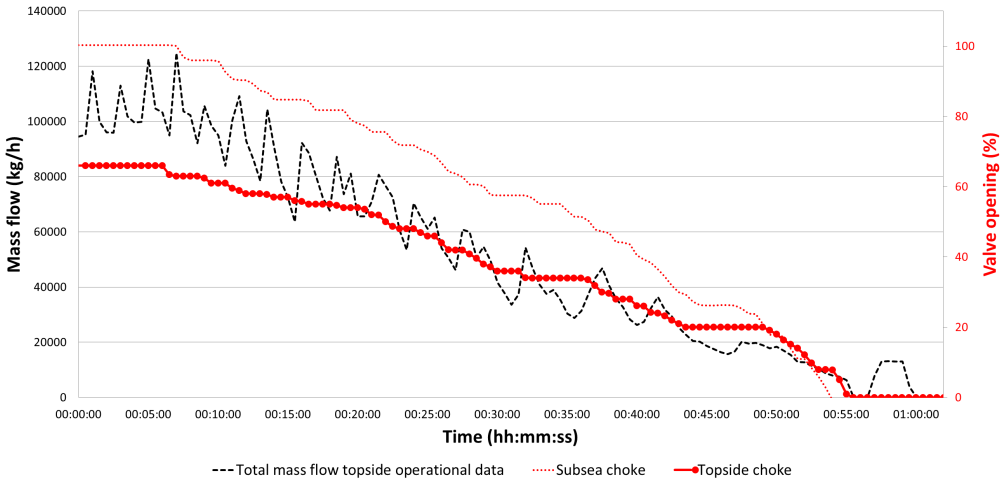

Figure 4.3: Recorded mass flow from production. The left vertical axis shows the mass flow in kg/h and the right vertical axis shows the percentage of the valve openings.

The simulated case, represented in 4.4, shows a constant mass flow before the valves start to close. Before the start of the sequence the mass flow is 120 300 kg/h and decreases slowly in the beginning of the shut-down procedure. As the sequence progresses the flow decreases faster. The fluctuations seen in the operational data are not seen in the simulation.

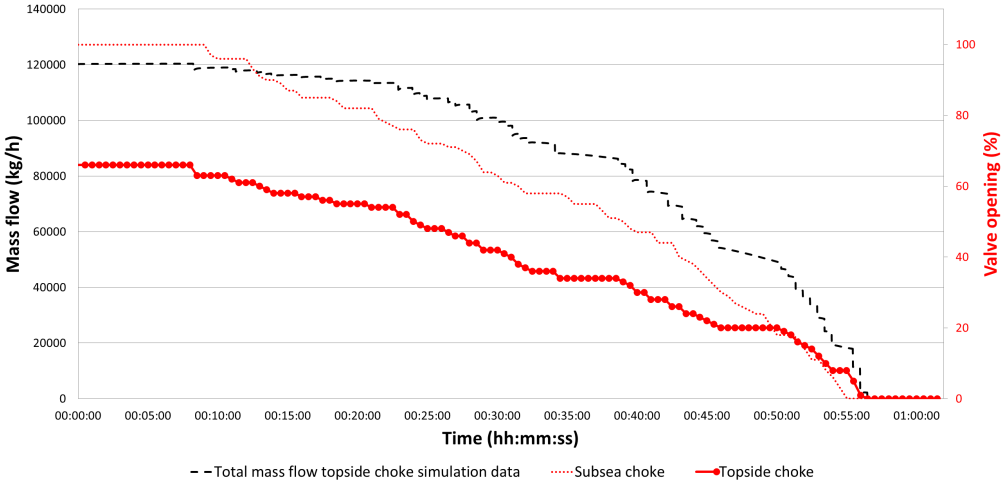

Figure 4.4: Mass flow from simulation. The left vertical axis shows the mass flow in kg/h and the right vertical axis shows the percentage of the valve openings.

In general, the pressure difference over the flowline is relatively constant for the operational data, while this is not the case for the simulation. The mass flow decreases in a relative constant rate than in the simulation.

4.3 Start-up scenario

Figures 4.5 to 4.8 present the result from the start-up scenario, both for the production data from the existing reservoir of choice as well as for the simulations.

Figure 4.5 and 4.6 show the pressure at different locations in the system together with the valve opening for the subsea choke and one of the topside chokes. The second topside choke is closed during this scenario. The locations from where the pressure data is taken from are: the wellhead, downstream wellhead, upstream riserbase and upstream topside chokes.

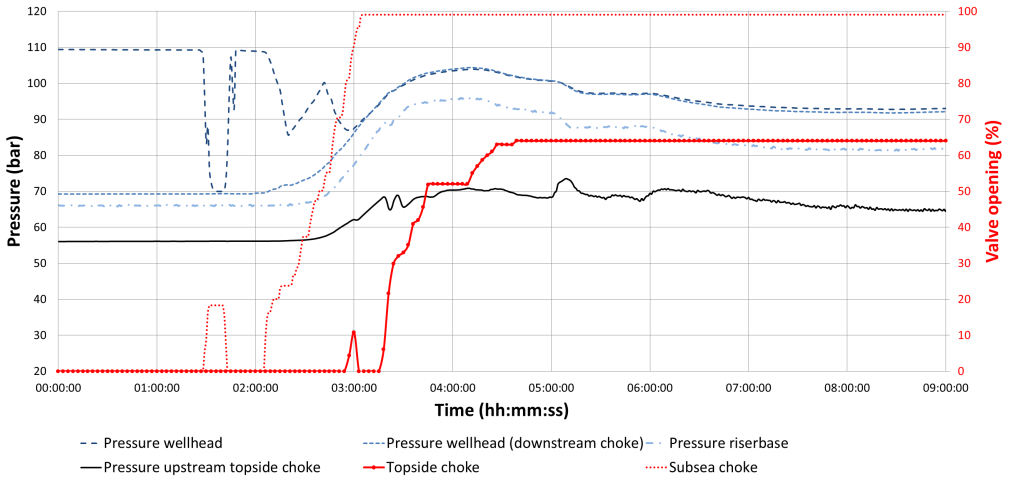

Figure 4.5: Recorded pressure over time during production start-up for the facility. The left vertical axis displays the pressure in bar and right vertical axis displays the valve opening in percentages.

As mentioned in section 3.4.2, the real production scenario of the start-up occurs six days after the shut-down of the production from the well. In figure 4.5 it is noticed that the wellhead pressure is 109.3 bar. Thus, the pressure in the well has increased from 100.6 bar to 109.3 bar during this period.

As seen in the graph (figure 4.5) both of the valves are opened and closed shortly before the start-up procedure of each valve has begun. In the same time as the subsea choke opens for the first time, the wellhead pressure is decreasing rapidly and meets the pressure at the other side of the subsea choke. The reason to the short opening of both of the chokes could simply be to test that the chokes and actuators works as intended.

When the subsea choke opens again, and the start-up procedure begins, the wellhead pressure decreases again. When the valves continue to open the pressure downstream the wellhead, in the riser base and upstream the topside chokes increases. When the chokes are open to their target actuator position, the pressure tend to level out and reaches steady state.

During the simulation of the start-up sequence, no consideration was taken to the first rapid opening of the chokes which is seen in the production data. The result of the simulated start-up procedure is shown in figure 4.6.

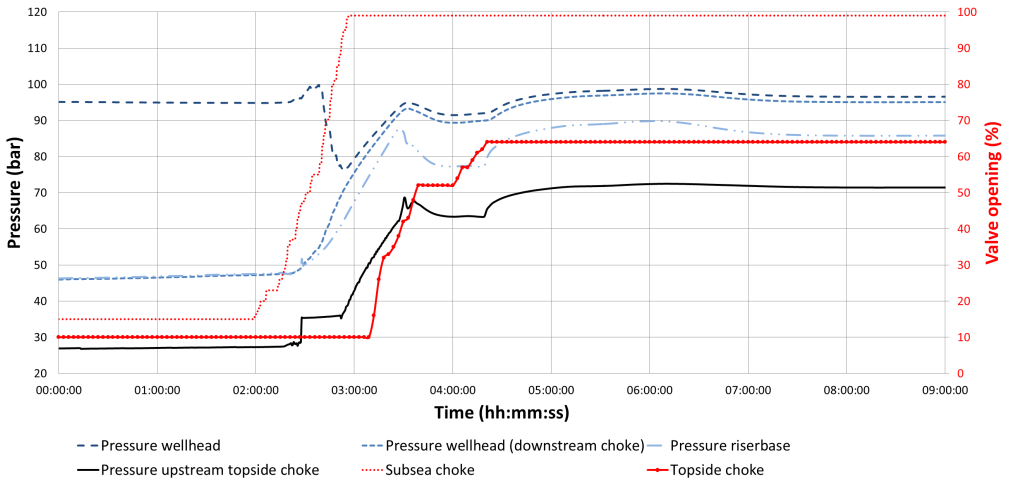

Figure 4.6: Result for the pressure over time for the start-up simulation. The left vertical axis displays the pressure in bar and right vertical axis displays the valve opening in percentages.

As seen in the graph (figure 4.6), the pressure downstream the subsea choke, the riserbase pressure and the pressure upstream the topside chokes are not steady from the beginning of the start-up. It was mentioned in section 3.4.2 that the simulation had stability issues when the flow reached below a certain limit. For the same reason, the pressures in the start-up scenario are not completely steady at the beginning. During many of the simulations where the flow was low, convergence problems were discovered before reaching a steady state condition. Trials with different step size in the dynamic integrator were executed and in most of the cases back flow of both liquid and gas could be seen in the flowline and in the riser. When the changes in the direction of the flow and the rapid changes in mass and volume become very large the solution in most of the cases crashed. In the final simulation a step size of 1 second was used.

The mass flow during the start-up procedure from the real scenario and from the simulated scenario are shown in figure 4.7 and figure 4.8 respectively. The recorded data, shown in figure 4.7, shows an unsteady behaviour in the mass flow upstream the topside chokes. This behaviour can be an indication of slugging of the flow. In the graph, a mass flow upstream the topside chokes can be seen during the time when both of the chokes are closed. The multiphase meter has recorded a gas flow

during this time, and no liquid flow. This is assumed to be a misreading by the multiphase meter.

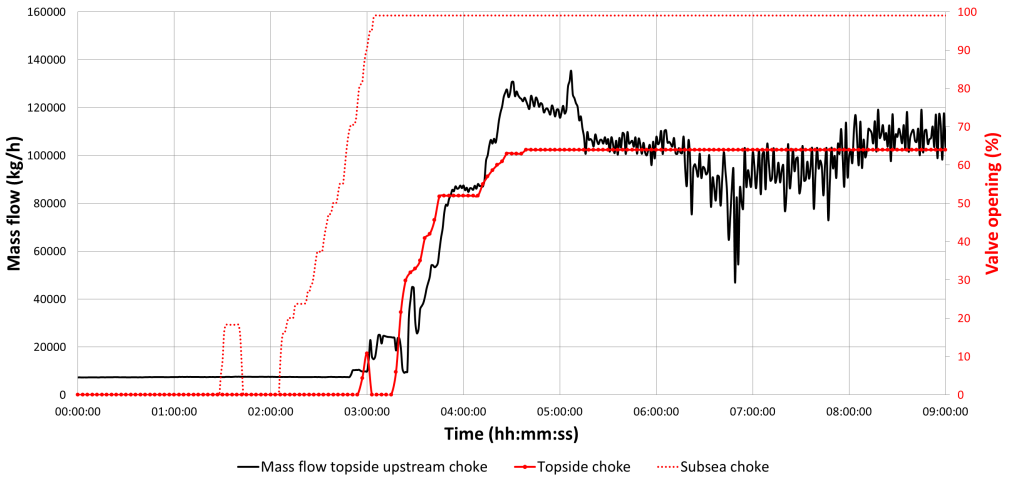

Figure 4.7: Recorded mass flow over time during production start-up for the facility. The left vertical axis shows the mass flow in kg/h and the right vertical axis shows the percentage of the valve openings.

The mass flow in the graph in figure 4.8 is seen to be more stable than the operational data. Before the beginning of the start-up, when the subsea choke is 15% opened and the topside choke is 10% opened, the average topside mass flow is 53.0 kg/h. A rapid decrease in the mass flow upstream the topside chokes can be seen in the end of the opening procedure.

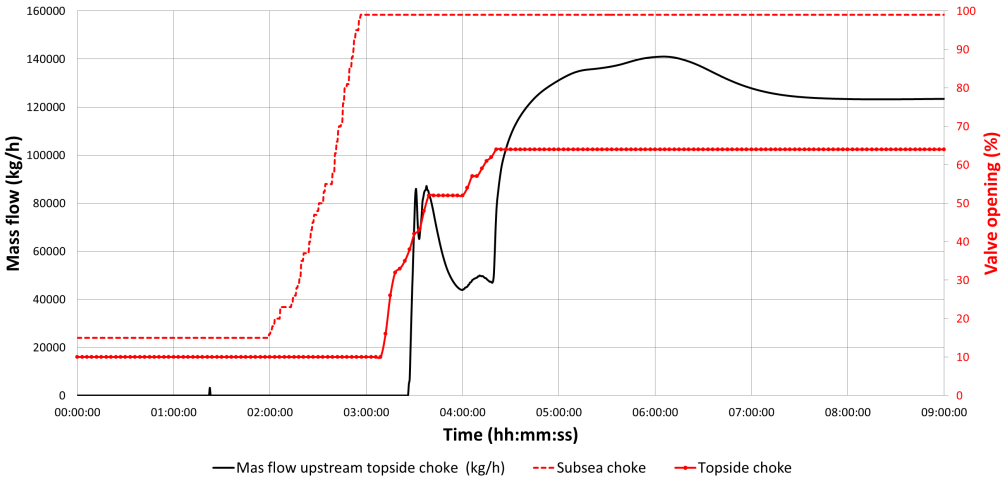

Figure 4.8: Mass flow over time from the start-up simulation. The left vertical axis shows the mass flow in kg/h and the right vertical axis shows the percentage of the valve openings.

The simulated process does not show the same kind of fluctuations as the real case data does. The fluctuations are probably due to slugging, which is not modelled in the simulation. In the real scenario the mass flow becomes approximately 110 000 kg/h after 9 hours, while in the simulated case the mass flow 123 400 kg/h after 9 hours.

4.3.1 Flow tracking in Hydraulics pipe segment

During simulations where the flow is low the flow downstream the flowline and the riser is seen to become negative during some periods. In the Hydraulics pipe segments the flow behaviour is tracked over the horizontal length of the pipe. Parameters which can be displayed along the Hydraulics pipe are, among others, mass flow, liquid holdup and pressure. During simulations which subsequently crashed large pikes of the flow rate, both positive and negative, could be seen in the flowline during short periods. The pikes changed amplitude and direction very fast and this can be seen as an indication of numerical errors in these solutions. The function of studying the flow behaviour is available in the Hydraulics pipe segment and not in the standard pipe segment in Aspen HYSYS.

4.4 Choke collapse

Simulations have been conducted according to section 3.4.3. Results are presented in form of mass flow and pressure over time in figures 4.9 to 4.14. As no operational data existed for a choke collapse, the results from simulations can not be validated as the shut-down and start-up scenarios.

4.4.1 Pressure change

Seen in figure 4.9 case A to C, which have upstream piping, a sudden and dramatic change in upstream topside choke pressure can be seen as the choke collapses. The pressure upstreams decreases. When the compressor has tripped and shuts down the pressure upstream the choke, downstream the choke and in the separator, starts to increase and equalise. It is also seen that the pressure at the risebase decreases for case A and B, in case C (figure 4.9c) this is the system boundary. In case A (figure 4.9a), where the boundary is upstream the well, no significant change can be seen at the wellhead.

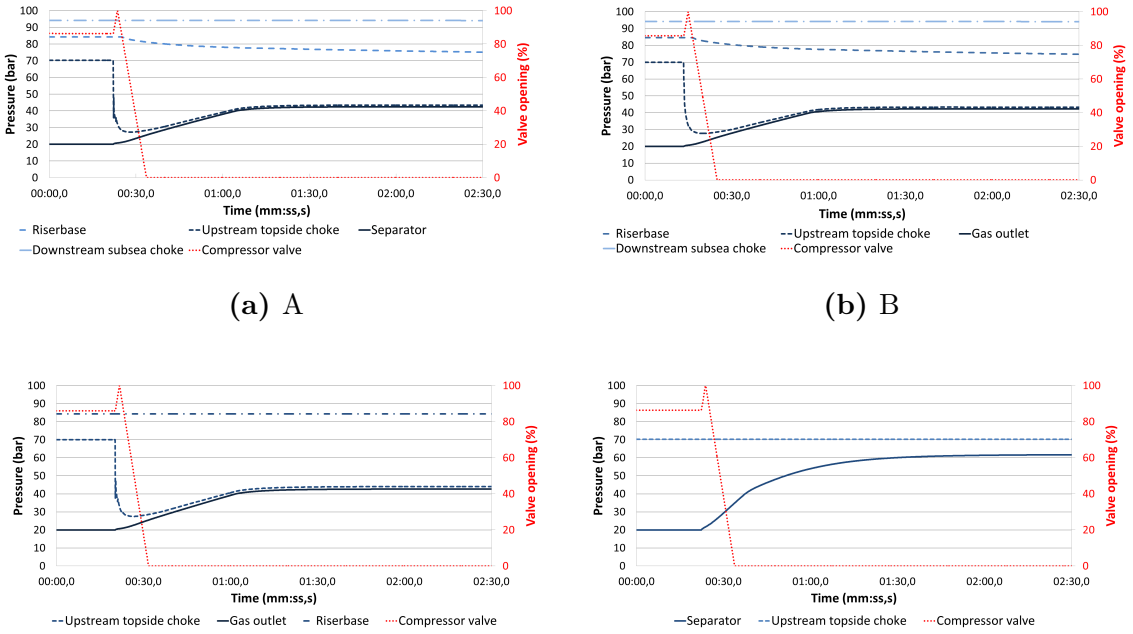

(a) A **(b)** B

(c) C **(d)** D

Figure 4.9: Pressure over time for the four simulated choke collapse cases. The left y-axis shows the pressure in bar and the right y-axis shows the valve opening in percentages.

For case D, figure 4.9d, a more rapid increase of the pressure and a higher end pressure is seen. The pressure upstream the choke is constant and therefore the pressure difference is only dependant upon the downstream equipment.

4.4.2 Flow through collapsed choke and riserbase

Seen in figure 4.10, the total mass flow through the collapsed topside choke is shown for each case. The graphs include the valve opening of the compressor valve. At first, when the choke collapses, there is a dramatic increase of the flow through the valve, see table 4.3 for the maximum mass flow. In case A to C the mass flow peaks and decreases rapidly before the compressor has tripped. In case D, figure 4.10d, the mass flow continues to increase slightly after the compressor has tripped to eventually slowly decrease. Case D also has the greatest maximum flow , as seen in table 4.3.

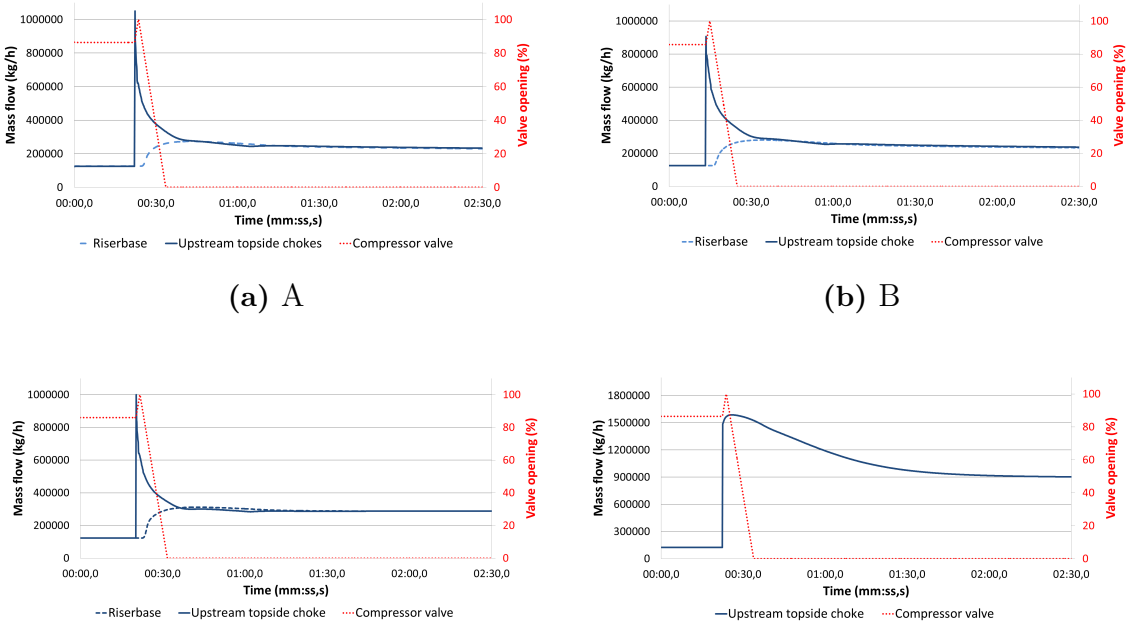

(a) A **(b)** B

(c) C **(d)** D

Figure 4.10: Total mass flow rate for the four choke collapse cases. Note the primary Y axis on figure 4.10d which ranges between 0 to 1 800 000 kg/h.

In case A to C, figure 4.10a to 4.10c, the dashed lines show the mass flow at the riserbase. The flow at the riserbase increases some seconds after the choke collapse, see table 4.3. The mass flow at the riserbase increases and stabilises to equal the mass flow at the collapsed choke.

Table 4.3: Peak flow and response time through the collapsed choke for each case.

	Peak flow after choke collapses (seconds)	Peak flow (kg/h)
A	0.2	1 049 570
B	0.4	906 223
C	0.2	999 565
D	3.3	1 586 760

4.4.3 Gas mass flow and venting to flare

As the choke collapses the flow in to the separator increases, also increasing the flow of the outlet streams from the separator. The gas outlet flow and the flow at the flare tip is shown in the figures 4.11 to 4.14. When the compressor valve trips gas starts to accumulate in the separator and in the piping upstream the compressor valve. Venting to the flare starts when the pressure in the separator reaches the set pressure of the PSVs. To cope with stability issues and to get relevant resolution over time for the relative short scenario a time step of 0.05 seconds was used.

In figure 4.11, the mass flow of the gas outlet for case A is shown. The compressor trips 1.5 seconds after the choke collapses. The PSVs open 42.4 seconds after the choke collapses.

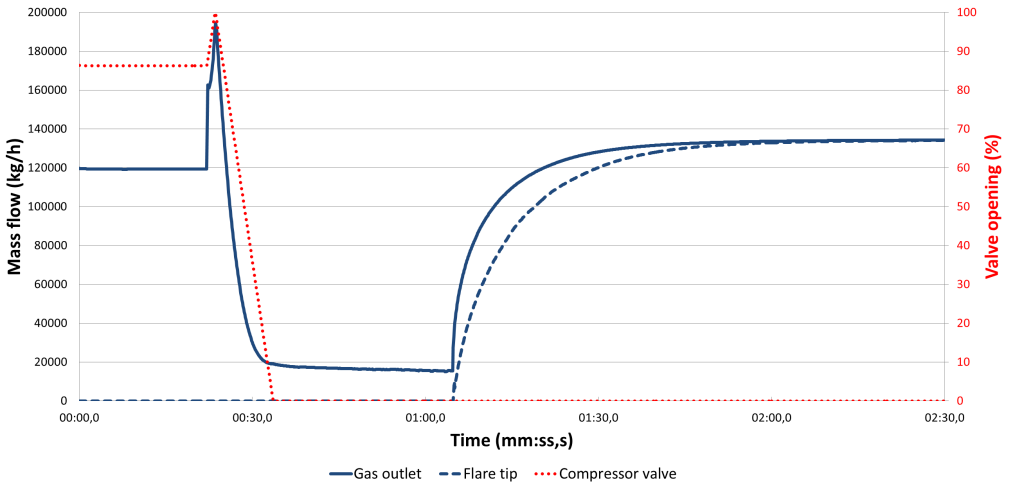

Figure 4.11: Gas flow for case A for the separator gas outlet and the flare tip. The small dotted line represents the opening percentage of the compressor valve.

In figure 4.12, the mass flow of the gas outlet for case B is shown. The compressor trips 1.8 seconds after the choke collapses. The PSVs open 44.3 seconds after the choke collapses.

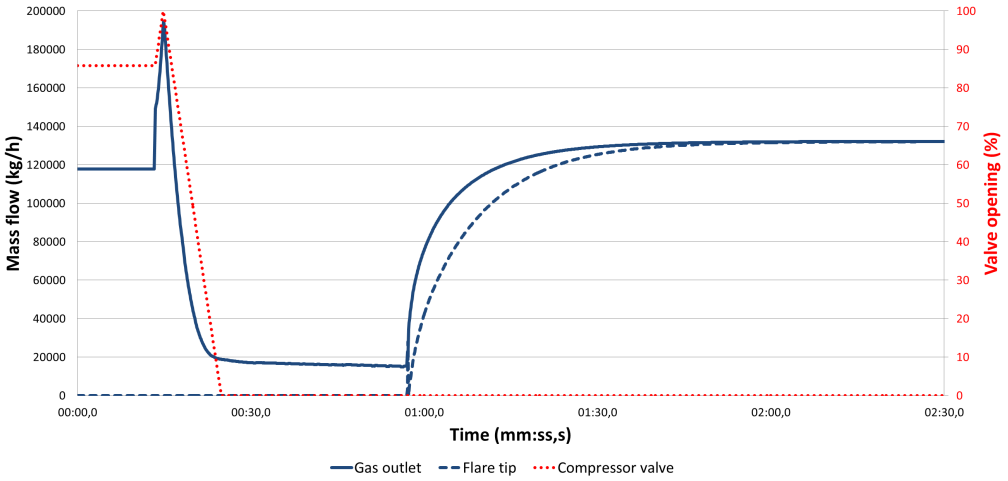

Figure 4.12: Gas flow for case B for the separator gas outlet and the flare tip. The small dotted line represents the opening percentage of the compressor valve.

In figure 4.13, the mass flow of the gas outlet for case C is shown. The compressor trips 1.5 seconds after the choke collapses. The PSVs open 41.5 seconds after the choke collapses.

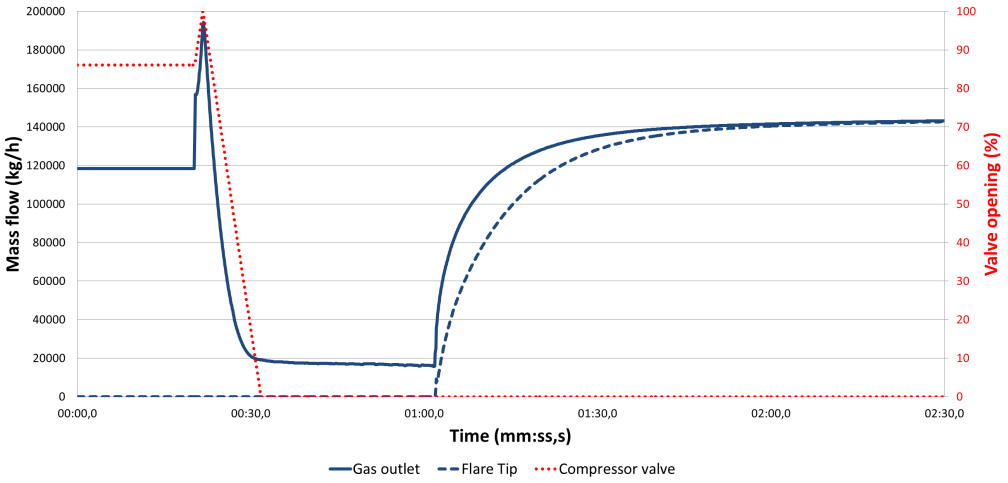

Figure 4.13: Gas flow for case C for the separator gas outlet and the flare tip. The small dotted line represents the opening percentage of the compressor valve.

In figure 4.14, the mass flow of the gas outlet for case D is shown. The compressor trips 1.6 seconds after the choke collapses. The PSVs open 15.2 seconds after the choke collapses.

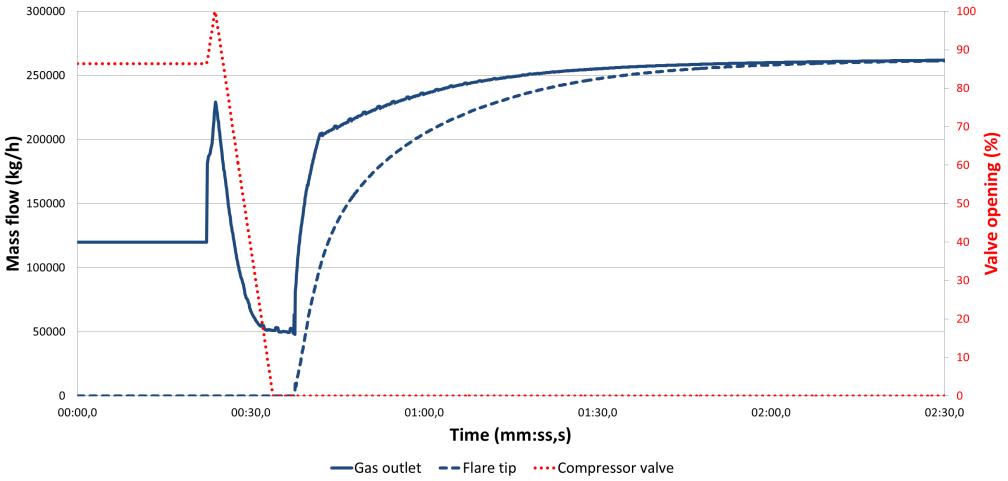

Figure 4.14: Gas flow for case D for the separator gas outlet and the flare tip. The small dotted line represents the opening percentage of the compressor valve.

The time between the choke collapse and the compressor trip is relatively constant for all cases. The time between the collapse and the opening of the PSVs are also relatively constant for case A to C, while case D's PSVs open after a shorter time. This is mainly due to the constant inlet pressure upstream the choke which gives a higher flow rate. The sudden change in increase of the gas outlet flow occurs when the PSVs reach 44 bar and are thereafter opened to 100%.

4.4.4 Stabilised collapsed choke flow

When the choke has collapsed and the venting to the flare system has stabilised (after approximately 2 minutes), differences in mass flow through the choke and the pressure of the separator are seen between the cases, table 4.4. An increase in mass flow is seen in decreasing model complexity, with largest change between case C and case D. The pressure in the separator in case A, B and C are under the rupture disc set pressure, 45.7 bar. In case D the pressure in the separator is 61.6 bar, which is 15.9 bar over the set pressure for the rupture disc and this would have resulted in disc rupture.

Table 4.4: Mass flow through the collapsed topside choke and pressure in the separator after approximately 2 minutes after the choke collapse.

	Mass flow topside choke (kg/h)	Separator pressure (bar)
A	232 675	42.4
B	237 502	42.3
C	287 930	42.7
D	908 512	61.6

5 Discussion

5.1 Model validation

The reservoir fluid characteristics change significantly between the production cases used for the model validation. For example, the GOR (table 3.2) varies from 234 to 381. In addition, the watercut changes remarkably from the earliest production case to the latest. It can be seen in table 3.2 that within a year, which is the time between case I and III, the watercut changes from 13% to 48%. This means, at during the latest production date, almost half of the produced liquid is water. The differences in fluid characteristics are considered to be appropriate to use for the model validation since it requires that the model gives good estimations for all cases.

5.1.1 Simulation results from the validation cases

The results of the riserbase pressure indicates that the model estimates the pressure drop in the flowline sufficiently. Since the pressure upstreams the topside chokes is set as a boundary condition the model will give a sufficient estimation of the pressure drop in the riser as well. Since the pressure is set as boundary conditions in the simulation the flow rate will be regulated to match the pressure boundaries. Therefore, the oil volume flow is used as one of the parameters in the validation. As seen in table 4.1 the oil flow from simulation case III deviates significantly from the actual value. By studying the boundary conditions for the cases (table 3.2) the watercut is almost half of the total liquid volume in case III. It is known, from internal documents, that the multiphase meter give more unreliable result the more water the flow consists of. Thus, a reasonable conclusion for the deviation in oil volume flow could be due to errors in the multiphase meter. On the other hand, the complexity with increased amount of water is problematic in the model as well. The calculation methods used to determine phase behaviour are similar for the multiphase meter and in Aspen HYSYS.

In general, the differences between the simulated results and the production data that can be seen in tables 4.1 to 4.2 and B.1 to B.4 are small. The model is considered to be valid for these three cases and hence can be considered to yield reliable

estimations for cases with similar characteristics. The only result that shows remarkable deviations between the actual data and the simulated data is the riserbase temperature. The following subsection contains a possible explanation.

5.1.2 Temperature measurements in production

In table B.4, showing the riserbase temperature, the percental difference between the operational values and the simulated results ranges between 4% to 22%. By comparing operational data of the temperature upstream the topside chokes and at the riserbase it is seen that the temperature is increasing over the riser for case I and II. For case III, the temperature decreases by 2 degrees over the riser.

Heat loss in the riser should occur since the ambient temperature, the water temperature, is lower than the stream temperature and no additional heating of the pipe occurs. The increase in temperature over the riser seems unlikely for this process and an error in one of the temperature meters is considered. Figure C.1 shows temperature profiles for the temperature meters by the riserbase and each topside choke. The data is taken for one production year and the first data point is from case I and the last data point is from case III. During periods when the temperature is low for one temperature meter (10 to 30 °C), the corresponding choke is closed.

Over a large part of the production year the temperature by the chokes, which are open, is higher than the temperature at the riserbase. From the graph in figure C.1 it can be concluded that it is the temperature meter at the riserbase which is measuring unreliable temperatures since both of the topside meters measure the same value when both opened. Due to this conclusion, the riserbase temperature from the production data was neglected in the validation. Instead, the validation of the temperature losses is done over the total system boundary. Since the temperature upstream the topside chokes (seen in table B.1) shows a deviation of maximum 3.1 °C the model is considered valid also with respect to heat losses.

5.2 Shut-down scenario

5.2.1 Differences in pressure drop for the production case and simulated case

In figure 4.1 and figure 4.2 it it seen that the pressure drop over the closed subsea choke is higher for the simulated data than for the operational data; 24.5 bar and 5.6 bar difference respectively. In the simulation, the pressures downstream the subsea choke and upstream the riserbase decrease during the shut-down sequence and when the chokes are completely shut, the pressure upstream the riserbase is slightly higher than the pressure downstream the subsea choke. In the production

case, the pressures at the same locations are maintained almost steady during the production shut-down.

The result for the simulated case can be described through the build-up of a fluid column in the pipe. As the fluids slow down in the downhill sloped flowline the static pressure will, by Bernoulli's equation, be highest in the lowest part of the pipe and lowest in the upper part. Though, the real production case does not show these characteristics. By studying how the real flowline is built over the seabed terrain (figure 3.2) it can be seen that the flowline incline and decline minor but several number of times along the 20 km long stretch. When the flow rate starts to decrease during the shut-down sequence liquid will probably accumulate in the low points of the flowline. The possible explanation is that the accumulated liquid is moved to form an inverted siphon (or plumber's trap) of gas with higher pressure. If this happens in all the minor low points in the flowline it will contribute to a static head leading to a major static pressure difference. These minor declinations and inclinations are not modelled, and this could be the explanation to why the results for the pressure diverge significantly between the production data and the simulation.

By studying figure 4.1 and figure 4.2, it is seen that the pressure drop over the riser is about 4 bar lower in the simulation data than the pressure drop in the production data. This could have the same explanation as for the pressure drop result for the flowline. Since the riser has a S-shaped curvature liquid will accumulate in the low point of the curvature, as an inverted siphon too. The gas with higher pressure at the riserbase forces the liquid upwards in the riser and two liquid columns will be formed. The columns will lead to an increased pressure at the riserbase. The model do not show this behaviour, resulting in a lower pressure difference over the riser.

5.2.2 Slugging effects

As seen in figure 4.3 and 4.4 the mass flow in the production data fluctuates heavily in contrast to the simulation results. As mentioned in section 4.2 this is probably due to slugging in the riser. This dynamic effect would be of interest to model and simulate due to its effect on the separator stage performance. The pipe model used predicts flow regimes which only purpose is to find a suitable pressure drop correlation. A more advanced tool to include slugging and connection to other equipment would be preferable in HYSYS.

5.2.3 Effect of valve characteristics

Another significant difference between the operational data and the simulations is the rate with which the flow decreases. A more linear decrease is seen in figure 4.3 than in figure 4.4. The leading theory why the operational data and the simulation results deviate is the uncertainty of the valve C_V and its characteristics. As the

manufacturer method could not be used for evaluating the topside chokes and due to the limited number of data points for constructing the valve characteristic curve this is concluded to be the largest source of error for the deviation.

5.3 Start-up scenario

As mentioned in the methodology section, the model had great problems handling low flows. Simulations that were initialised with all of the chokes closed did not converge. For the simulation to converge, a flow through the system was required. Several days of simulations were needed to find a solution for the convergence problems. The choke openings at 15 % and 10 % for the subsea choke and topside choke respectively gave the lowest flow that could be maintained without the simulation to crash. Due to the instabilities, the final simulation could not reach steady state before the start of the start-up procedure. This could be a source of error and it is discussed further in this section. Due to the convergence problems, the subsequent discussion is focused on the dynamic behaviour prior to the absolute values of the results.

5.3.1 Pressure in the system during start-up scenario

As seen in figure 4.6 the wellhead pressure starts to increase in the middle of the start-up sequence of the subsea choke. After the pressure increase, the wellhead pressure decreases in the end of the opening sequence of the subsea choke. This behaviour can be seen also in the pressure data from the production case. Both graphs show a decrease in the wellhead pressure followed by an increase when the subsea choke is almost at its final actuator position (99%). A potential explanation for the decrease in pressure could be that gas has accumulated at the top of the well while liquid is at the bottom of the riser. When the subsea choke opens the gas will move through the choke and cause the pressure to equalise rapidly. When the more dense liquid starts to move through the choke the pressure will increase again. This behaviour is also seen in the simulation, though it is unknown if it is due to the same phenomena.

The wellhead pressure downstream the subsea choke has a slightly higher value than the pressure at the riserbase before the start-up in the simulated scenario while there is a pressure drop over the flowline at the same time in the production data. The reason for this divergence is the same as explained in section 5.2; that the model gives a static pressure contribution higher than the reality because the simplification of the routing of the flowline. The accumulation of liquid in the low points of the flowline gives the static pressure contribution in the real production case.

As mentioned earlier, the pressure in the system is not steady when the start-up sequence begins. Because of that, the pressure from the simulated data is lower in all parts of the system compared to the production data when the start-up sequence

begins. Though, the pressure graphs show a similar behaviour for the pressure with a peak of the pressures followed by an adjustment period where the pressure settles out. The pressures at the different locations in the simulation are, after the settling time, similar to the pressures recorded from the production data. At the most, the pressure differs with 6 bar in the simulated data compared to the production data.

5.3.2 Mass flow in the system during start-up scenario

An initial comparison of the graphs for the mass flow in the start-up scenario (figure 4.7 and figure 4.8) shows large fluctuations in the production data while no fluctuations can be seen in the simulated data. The fluctuations indicate that there is slugging in the flow. The pressure drop models used in the software predict the flow regimes and use the proper equation to solve the pressure drop for each flow regime. Though, the model can not predict the behaviour of each phase separately and the slugging is not seen in the mass flow from the simulation.

The multiphase meter measuring the flow rate at the production facility is located upstream the topside choke. Data for the mass flow in the simulation is logged at the same position in the model; upstream the topside chokes. It is seen in figure 4.8 that the mass flow increases rapidly from zero to 85 000 kg/h when the topside choke reaches a opening position of about 40%. The production data shows a more continuous increase in flow rate during the start-up sequence of the topside choke.

The reason for the varied behaviour in the flow rates could be the valve characteristic for the topside chokes. The characteristic implemented in the model (shown in figure 3.7) is an approximation based on a few known measurements. The valve characteristic is correlated to the C_V and thus the flow rate through the choke. The characteristic curve implemented in the model could be too flat for low choke openings and maybe have a higher slope for high choke openings than the characteristic curve of the real topside choke. The standardised ANSI/ISA method for calculating the valve characteristic is also a source of error since the real manufacturer method was not implemented in HYSYS.

In the simulated results an abrupt decrease in the mass flow can be seen in figure 4.8 after about 4 hours. A similar behaviour of the pressure is shown at the same time (figure 4.6). This behaviour is not seen in the production data. The dip occurs at the same time as the topside choke for about 20 minutes stays at the same opening position during the sequence. A possible explanation for this may be that the topside choke opening sequence proceeds rapidly until the 20 minute pause and the quick choke opening could have contributed to a momentum change through the system. The momentum would give a rapid increase in the volume flow and when the choke is at the same opening position a longer period the momentum would wane and make both the mass flow and the pressure to decrease. The same behaviour could explain the curves in the mass flow graphs at a later time of the start-up sequence of the topside choke. The valve characteristics will give a higher effect in the flow rate at higher opening positions.

5.4 Choke collapse

As mentioned in section 4.4, the choke collapse simulation is of speculative nature. The result presented shows a minor difference between case A, B and C, while case D deviates the most. The result is more or less straight forward, the dampening effect of the volume, frictional loss and static pressure loss decrease with decreased model complexity. During this relatively short course of time, it can be seen that the riser is of greatest importance to get a reasonably same dynamic behaviour. The result is expected, especially when the riser is the closest upstream equipment to the topside facility with a significant volume.

5.4.1 Peak flow during choke collapse

As presented in 4.4.2 the flow increases dramatically directly after the choke collapses in all cases. In case A, B and C the flow also decreases rapidly afterwards resulting in the flow peak shown in figure 4.10. This is due to the upstream volume which "vents" to the downstream equipment. For case D, there are no upstream volumes due to the system boundary which is set to constant pressure and temperature. This also results in the major difference in flow when the PSVs vent to the flare between the cases.

Case B shows a lower peak flow and slightly longer time between the collapse and tripping time of the compressor than case A. Case C also shows a lower peak flow than case A. This does not correspond with the theory of less pressure loss with less complex model. One idea why this behaviour is seen is that it can be due to the sampling during the simulations. Data have been sampled every other time step. If the flow has peaked between two sampled time steps, the true value of the peak might have been missed.

5.4.2 Requirements of pressure safety equipment

The pressure in the system during the cases is presented in figure 4.9. Case A, B and C show the same behaviour regarding the pressure upstream the choke and in the separator. The end pressure in the separator, seen in table 4.4, is also in the same order of magnitude. Case D shows a significantly higher end pressure. As mentioned in 4.4 this pressure is 15.9 bar greater than the set pressure of the rupture disc. In regular evaluation of the flow through the PSVs, simulations are conducted without taking the upstream piping into account, in accordance with case D. This might be the reason why a rupture disc have been installed from the first place; to cope with the high pressure when setting the system boundary at the topside choke. This might indicate that the separator do not need to be rebuilt if additional wells were to be tied to the platform, reducing investment cost.

5.4.3 Compressor trip and choke collapse imitation

As presented in section 4.4.3, the time between the choke collapse and the compressor trip is between 1.5 and 1.8 seconds. As no recorded data from the platform where the compressor trips of this reason is known, it can be speculated if the change in speed and flow though the compressor would occur as quickly as in the simulations. As the compressor already is working at high capacity this event will probably be short and in the range of seconds, thus the time between the collapse and trip can be seen as reasonable. Another factor which can have influenced how accurate the result is in accordance to a real choke collapse is the instantaneous opening of the choke valves. Is an instantaneous opening representable for a choke collapse? Probably a quick and fast increase of the C_V may had been better and more representative for a choke collapse. Still, no information of how this quick increase looks like in reality was found and the focus have instead been consistent in simulations.

5.4.4 Sufficient model complexity

As the above discussion implies, the differences between the cases are notable. Though, the difference between the three cases containing upstream piping and case D shows how important the choice of system boundary is. The flow and pressure after the collapse, presented in table 4.4, show that case B and C have a 2.1% and 23.7% higher flow than case A respectively. This is relative small differences when compared to the flow in case D, which is 290.5% higher. When evaluating fast dynamic scenarios, such as choke collapses and the safety equipment it might not be necessary to extend the model to include all upstream equipment. As indicated, case C is sufficient to see the overall behaviour and to evaluate the size of the PSVs. The extra complexity when adding the flowline is seen, if not looking for a much more precise solution which increases the simulation time significantly, as unnecessary.

5.5 Additional sources of errors in the model setup

5.5.1 Design of flowline and riser

The pressure drop correlation models implemented in the flowline and the riser are based on theoretical knowledge about the correlations and on simulations performed in an early stage of the project. Though, the pressure correlation models could be a source of error in the model for prediction of the pressure loss. For example, the Beggs and Brill is overpredicting the pressure drop in downward inclined flows. It is still implemented in the riser where the pipe is downwardly inclining, though the pressure losses in the simulations do not deviate from the production data for the validation results. The pressure drop correlation models might have an impact on the other scenarios as the shut-down or start-up. Different models are not tested for

these cases in this study. It can also be discussed whether the riser is modelled too simple and should be modelled more rigorously than only in three segments. The model of the simplified riser was implemented since the focus was at the flowline at the start of the project and to model it more rigorously than the riser. As the model complexity increases more equations need to be solved which increases time required for simulations, these are two factors that need to be balanced.

5.5.2 Ambient temperature

The ambient temperature is set to 5°C for all modelled segments, also for the well. Since the well is drilled several meters down in the sea bottom, it is unreasonable to have this low temperature that far down in the ground close to the reservoir. This is something that was noticed after the simulations had been performed. A more reasonable ambient temperature for the well would give better predictions for pressure drop and temperature drop for the flow. Though, the main reason to model the well was to include the volume of the bore hole during the dynamic simulations, and the pressure drop in the bore hole is not as important for the results.

6 Conclusions

The work has been focused on simulating subsystems of an oil and gas production system. Models have been formulated to contain parts like the well, flowline, riser and topside equipment. At stationary conditions, the result and discussion conclude that long dynamic scenarios are harder to evaluate properly. This might be due to instability issues with the model and solver used and due to accumulated effects of elevation which were not included in the models. Shorter dynamic scenarios have been modelled with greater success.

Answers on research questions:

1. *Will dynamic simulations of the subsea system have effects on design and sizing of topside downstream equipment?*

It is concluded that dynamic simulations of subsea systems provide an extra insight to evaluation of safety equipment such as chokes, PSVs and other units of the topside facility such as separators and compressors. Furthermore, dynamic simulation where parts of the upstream equipment are included is useful for minimising amount of and size of safety equipment and thereby reduce weight and capital cost.

2. *To what extend can the model/models be simplified? For the system to be representable and valid, how coarse can the resolution be?*

It is necessary to consider the increased accuracy against the extra time required for modeling and simulations as the model complexity increases. After evaluating the effect of model complexity it is shown that the model can be simplified to contain adjacent upstream equipment for an improved dynamic evaluation of the topside system.

3. *Can an efficient framework for simulations of similar systems be expressed?*

A specific proposal for a framework have not been formulated, though some major recommendations for similar simulations are provided: model valve and valve characteristics thoroughly; evaluate how much the system is affected by small accumulated changes, like topography of the sea floor; start with a stationary solution of the system to get possible boundaries for less complexed dynamic simulations.

References

1. Bai, Y. & Bai, Q. in *Subsea Engineering Handbook* (eds Bai, Y. & Bai, Q.) 3–25 (Gulf Professional Publishing, Boston, 2010). ISBN: 978-1-85617-689-7. doi:http://dx.doi.org/10.1016/B978-1-85617-689-7.10001-9. <http://www.sciencedirect.com/science/article/pii/B9781856176897100019>.
2. A Brief History of Offshore Oil Drilling. *BP Deep Horizon Oil Spill Commission.* <www.cs.ucdavis.edu/~rogaway/classes/188/materials/bp.pdf> (2010).
3. Chakrabarti, S., Halkyard, J. & Capanoglu, C. *Chapter 1 - Historical Development of Offshore Structures* (ed CHAKRABARTI, S. K.) 1–38. ISBN: 978-0-08-044381-2. doi:http://dx.doi.org/10.1016/B978-008044381-2.50004-7. <http://www.sciencedirect.com/science/article/pii/B9780080443812500047> (Elsevier, London, 2005).
4. Schempf, F. J. ANNIVERSARY SPECIAL The history of offshore: developing the E&P infrastructure. *Offshore* **64,** 20–35. ISSN: 00300608 (2004).
5. Pratt, J. A., Priest, T. & Castaneda, C. J. *Offshore Pioneers* (eds Pratt, J. A., Priest, T. & Castaneda, C. J.) ISBN: 978-0-88415-138-8. doi:http://dx.doi.org/10.1016/B978-088415138-8/50037-5. <http://www.sciencedirect.com/science/article/pii/B9780884151388500375> (Gulf Professional Publishing, Burlington, 1997).
6. Devold, H. *Oil and Gas Production Handbook, An introduction to oil and gas production* ISBN: 978-82-997886-2-5 (ABB, Oslo, 2010).
7. Bai, Q. & Bai, Y. in *Subsea Pipeline Design, Analysis, and Installation* (ed Bai, Q. B.) 3–21 (Gulf Professional Publishing, Boston, 2014). ISBN: 978-0-12-386888-6. doi:http://dx.doi.org/10.1016/B978-0-12-386888-6.00001-8. <http://www.sciencedirect.com/science/article/pii/B9780123868886000018>.
8. Bratland, O. *Pipe Flow 2: Multi-phase Flow Assurance* 2nd ed. (ed Bratland, O.) ISBN: 978-616-335-926-1 (Ove Bratland, Burlington, 2013).
9. in. *PVT and Phase Behaviour of Petroleum Reservoir Fluids* (ed Danesh, A.) 1–31 (Elsevier, 1998). doi:http://dx.doi.org/10.1016/S0376-7361(98)80023-X. <http://www.sciencedirect.com/science/article/pii/S037673619880023X>.

10. Bai, Y. & Bai, Q. in *Subsea Engineering Handbook* (eds Bai, Y. & Bai, Q.) 27–62 (Gulf Professional Publishing, Boston, 2010). ISBN: 978-1-85617-689-7. doi:http://dx.doi.org/10.1016/B978-1-85617-689-7.10002-0. <http://www.sciencedirect.com/science/article/pii/B9781856176897100020>.

11. Bai, Y. & Bai, Q. in *Subsea Engineering Handbook* (eds Bai, Y. & Bai, Q.) 571–632 (Gulf Professional Publishing, Boston, 2010). ISBN: 978-1-85617-689-7. doi:http://dx.doi.org/10.1016/B978-1-85617-689-7.10019-6. <http://www.sciencedirect.com/science/article/pii/B9781856176897100196>.

12. Fang, H. & Duan, M. in *Offshore Operation Facilities* (eds Fang, H. & Duan, M.) 341–536 (Gulf Professional Publishing, Boston, 2014). ISBN: 978-0-12-396977-4. doi:http://dx.doi.org/10.1016/B978-0-12-396977-4.00003-2. <http://www.sciencedirect.com/science/article/pii/B9780123969774000032>.

13. Sinnott, R. K. & Towler, G. *Chemical Engineering Design (2nd Edition)* English. ISBN: 9780080966595;0080966594; (Elsevier Science, 2014;2013;).

14. Campbell, J. M. *Gas Conditioning and Processing* 8th (ed Hubbard, R. A.) ISBN: 0-9703449-0-2 (John M. Campbell and Company, Norman, Oklahoma U.S.A).

15. Smith, P. & Zappe, R. in *Valve Selection Handbook (Fifth Edition)* (eds Smith, P. & Zappe, R.) Fifth Edition, 7–45 (Gulf Professional Publishing, Burlington, 2004). ISBN: 978-0-7506-7717-2. doi:http://dx.doi.org/10.1016/B978-075067717-2/50002-X. <http://www.sciencedirect.com/science/article/pii/B978075067717250002X>.

16. Skousen, P. L. *Valve handbook* 3rd. English. ISBN: 9780071743891;0071743898; (McGraw-Hill, New York, 2011;2012;).

17. Bai, Y. & Bai, Q. in *Subsea Engineering Handbook* (eds Bai, Y. & Bai, Q.) 703–761 (Gulf Professional Publishing, Boston, 2010). ISBN: 978-1-85617-689-7. doi:http://dx.doi.org/10.1016/B978-1-85617-689-7.10022-6. <http://www.sciencedirect.com/science/article/pii/B9781856176897100226>.

18. Jamaluddin, A. & Kabir, C. Flow assurance: Managing flow dynamics and production chemistry. *Journal of Petroleum Science and Engineering* **100,** 106–116. ISSN: 0920-4105 (2012).

19. Guo, B., Song, S., Ghalambor, A. & Lin, T. R. in *Offshore Pipelines (Second Edition)* (ed Lin, B. G. S. G. R.) Second Edition, 179–231 (Gulf Professional Publishing, Boston, 2014). ISBN: 978-0-12-397949-0. doi:http://dx.doi.org/10.1016/B978-0-12-397949-0.00015-7. <http://www.sciencedirect.com/science/article/pii/B9780123979490000157>.

20. Bai, Y. & Bai, Q. in *Subsea Engineering Handbook* (eds Bai, Y. & Bai, Q.) 331–347 (Gulf Professional Publishing, Boston, 2010). ISBN: 978-1-85617-689-7. doi:http://dx.doi.org/10.1016/B978-1-85617-689-7.10012-3. <http://www.sciencedirect.com/science/article/pii/B9781856176897100123>.

21. Bai, Y. & Bai, Q. in *Subsea Engineering Handbook* (eds Bai, Y. & Bai, Q.) 451–481 (Gulf Professional Publishing, Boston, 2010). ISBN: 978-1-85617-689-7. doi:http://dx.doi.org/10.1016/B978-1-85617-689-7.10015-9. <http://www.sciencedirect.com/science/article/pii/B9781856176897100159>.

22. Bai, Y. & Bai, Q. in *Subsea Pipelines and Risers* (eds Bai, Y. & Bai, Q.) 277–316 (Elsevier Science Ltd, Oxford, 2005). ISBN: 978-0-08-044566-3. doi:http://dx.doi.org/10.1016/B978-008044566-3.50020-8. <http://www.sciencedirect.com/science/article/pii/B9780080445663500208>.

23. in. *Process Modelling and Model Analysis* (eds Hangos, K. & Cameron, I.) 3–18 (Academic Press, 2001). doi:http://dx.doi.org/10.1016/S1874-5970(01)80025-4. <http://www.sciencedirect.com/science/article/pii/S1874597001800254>.

24. Hyvärinen, L. *Chapter 1 - Basic concepts* (ed L., H.) 1–10. ISBN: 978-3-540-04943-2. doi:http://dx.doi.org/10.1007/978-3-642-87427-7. <http://link.springer.com.proxy.lib.chalmers.se/book/10.1007%5C%2F978-3-642-87427-7> (Springer Berlin Heidelberg, Geneva, 1970).

25. Cameron, I. & Ingram, G. A survey of industrial process modelling across the product and process lifecycle. *Computers Chemical Engineering* **32,** 420–438. ISSN: 0098-1354 (2008).

26. in. *Process Modelling and Model Analysis* (eds Hangos, K. & Cameron, I.) xiii–xvi (Academic Press, 2001). doi:http://dx.doi.org/10.1016/S1874-5970(01)80024-2. <http://www.sciencedirect.com/science/article/pii/S1874597001800242>.

27. Stephanopoulos, G. in *10th International Symposium on Process Systems Engineering: Part A* (eds Rita Maria de Brito Alves, C. A. O. d. N. & Biscaia, E. C.) 149–155 (Elsevier, 2009). doi:http://dx.doi.org/10.1016/S1570-7946(09)70246-9. <http://www.sciencedirect.com/science/article/pii/S1570794609702469>.

28. in. *Process Modelling and Model Analysis* (eds Hangos, K. & Cameron, I.) 65–82 (Academic Press, 2001). doi:http://dx.doi.org/10.1016/S1874-5970(01)80028-X. <http://www.sciencedirect.com/science/article/pii/S187459700180028X>.

29. Barrufet, M. A. A brief introduction to equations of state for petroleum engineering applications. English. *Hart's Petroleum Engineer International* **71,** 81 (1998).

30. Peng, D.-Y. & Robinson, D. B. A New Two-Constant Equation of State. *Industrial & Engineering Chemistry Fundamentals* **15,** 59–64 (1976).

31. in. *PVT and Phase Behaviour of Petroleum Reservoir Fluids* (ed Danesh, A.) 301–352 (Elsevier, 1998). doi:http://dx.doi.org/10.1016/S0376-7361(98)80031-9. <http://www.sciencedirect.com/science/article/pii/S0376736198800319>.

32. Beggs, D. & Brill, J. A Study of Two-Phase Flow In Inclined Pipes. English. *Journal of Petroleum Technology* **25.** <https://www-onepetro-org.proxy.lib.chalmers.se/journal-paper/SPE-4007-PA> (1973).

33. Payne, G. A., Palmer, C. M., Brill, J. P. & Beggs, H. D. Evaluation of Inclined-Pipe, Two-Phase Liquid Holdup and Pressure-Loss Correlation Using Experimental Data (includes associated paper 8782). English. *Journal of Petroleum Technology* **31,** 1198–1208 (1979).

34. Duns, H. & Ros, N. J. C. Vertical flow of gas and liquid in wells. English. *World Petroleum Congress,* 451–465 (1963).

35. *HYSYS 2004.2 Operations Guide* Aspen Technology (Cambridge, MA 02141-2201, USA, 2005).

36. Wadekar, V. V., Tian, Y. S. & T., K. *Two-phase pressure drop during flow boiling of hydrocarbon fluids* in *5th European Thermal-Sciences Conference* (2008).

37. Thomas, P. in *Simulation of Industrial Processes for Control Engineers* (ed Thomas, P.) 239–255 (Butterworth-Heinemann, Oxford, 1999). ISBN: 978-0-7506-4161-6. doi:http://dx.doi.org/10.1016/B978-075064161-6/50020-1. <http://www.sciencedirect.com/science/article/pii/B9780750641616500201>.

38. Feliu, J. A., Grau, I., Alos, M. A. & Macias-Hernandez, J. Match Your Process Constraints Using Dynamic Simulation. English. *Chemical Engineering Progress* **99,** 42 (2003).

39. Mokhatab, S. & Towler, B. F. Dynamic Simulation of Offshore Production Plants. English. *Petroleum Science and Technology* **25,** 741–757 (2007).

40. Product Marketing, A. T. I. *An Integrated Approach to Modeling Pipeline Hydraulics in a Gathering and Production System* 2015.

41. *ANSI/ISA-75.01.01 (IEC 60534-2-1 Mod)-2007 Flow Equations for Sizing Control Valves* 2007.

.

A Appendix A

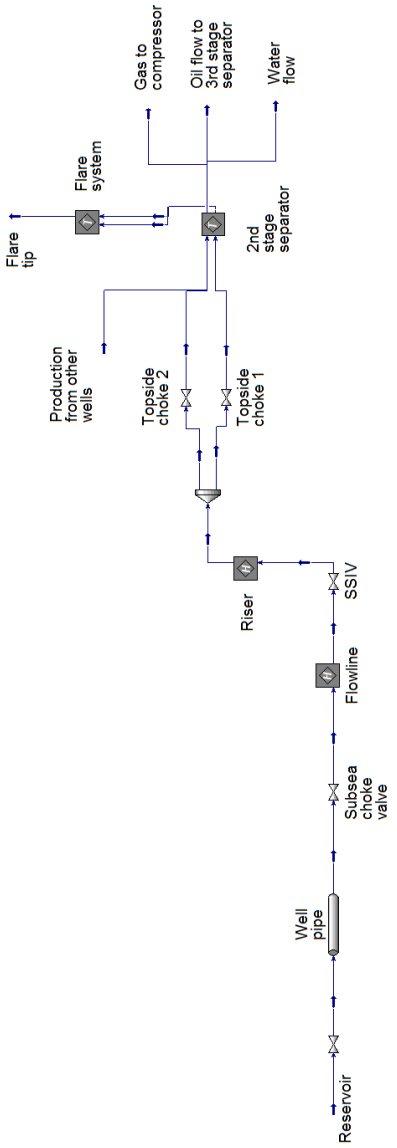

Figure A.1: Flowsheet of the complete model.

B Appendix B

B.1 Model validation

Table B.1: Validation result of the topside choke temperature.

Upstream topside choke temperature (°C)				
	Actual	Model	Diff	Diff (%)
I	55.4	57.9	2.5	4.5
II	65.4	64.6	-0.7	-1.1
III	64.4	61.3	-3.1	-4.9

Table B.2: Validation result of the GOR topside.

GOR				
	Actual	Model	Diff	Diff (%)
I	381	392	10.7	2.8
II	234	240	6.7	2.8
III	301	301	0.0	0.0

Table B.3: Validation result of the Watercut topside.

Watercut				
	Actual	Model	Diff	Diff (%)
I	0.126	0.122	-0.004	-2.929
II	0.354	0.347	-0.007	-1.840
III	0.478	0.467	-0.011	-2.289

Table B.4: Validation result of the riserbase temperature.

Riser base temperature (°C)				
	Actual	Model	Diff	Diff (%)
I	50.6	61.7	11.1	21.9
II	64.9	70.2	5.3	8.2
III	66.4	69.1	2.7	4.0

B.2 Choke collapse

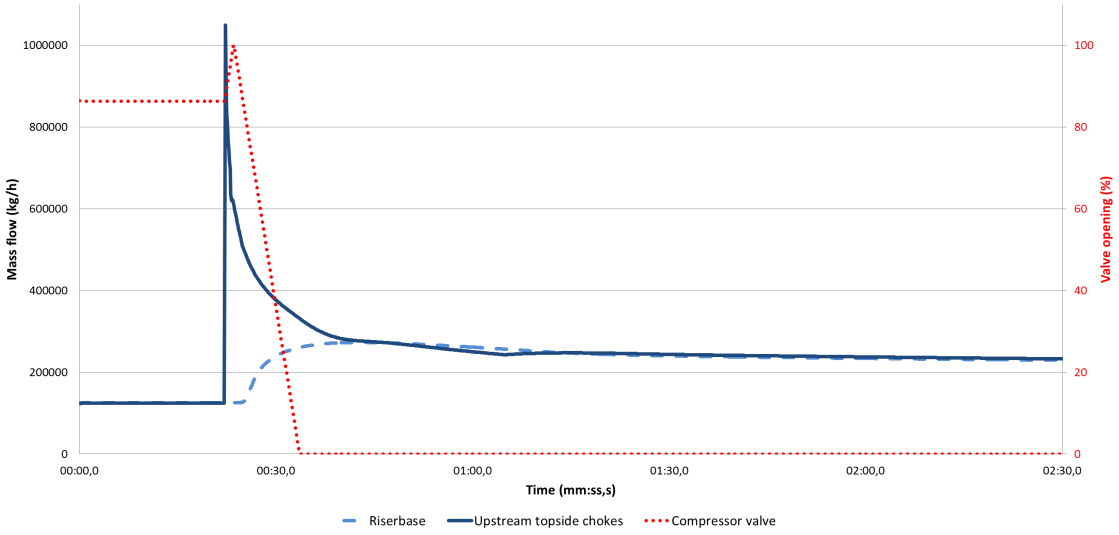

Figure B.1: Total mass flow rate for the choke collapse case A.

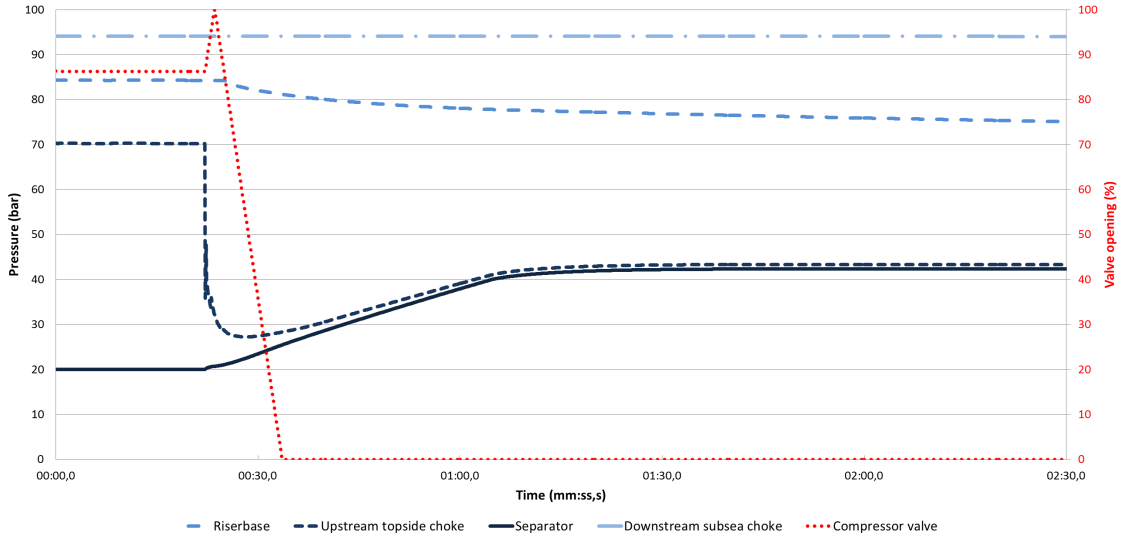

Figure B.2: Pressure for the choke collapse case A.

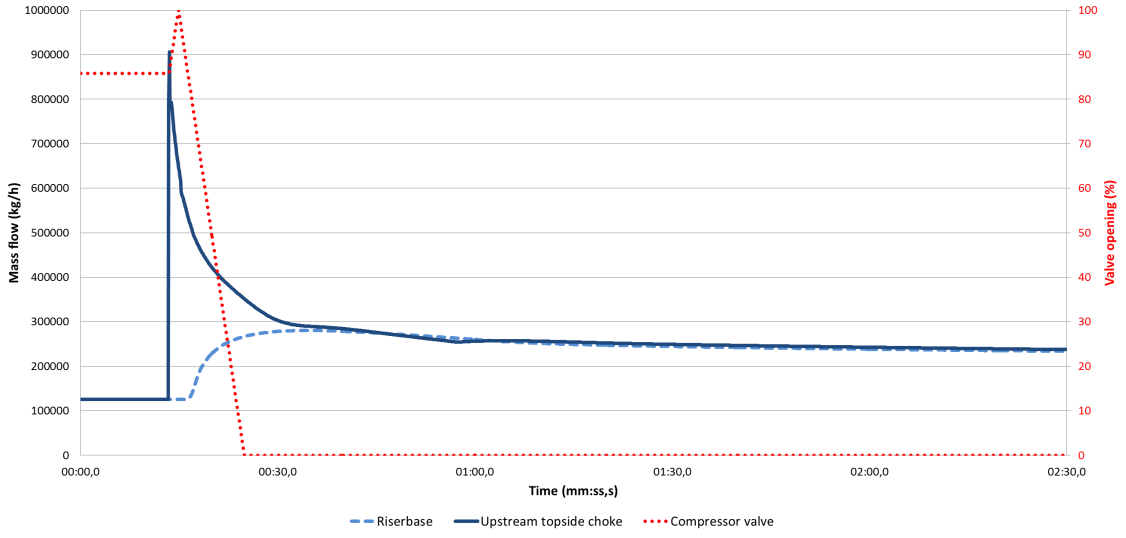

Figure B.3: Total mass flow rate for the choke collapse case B.

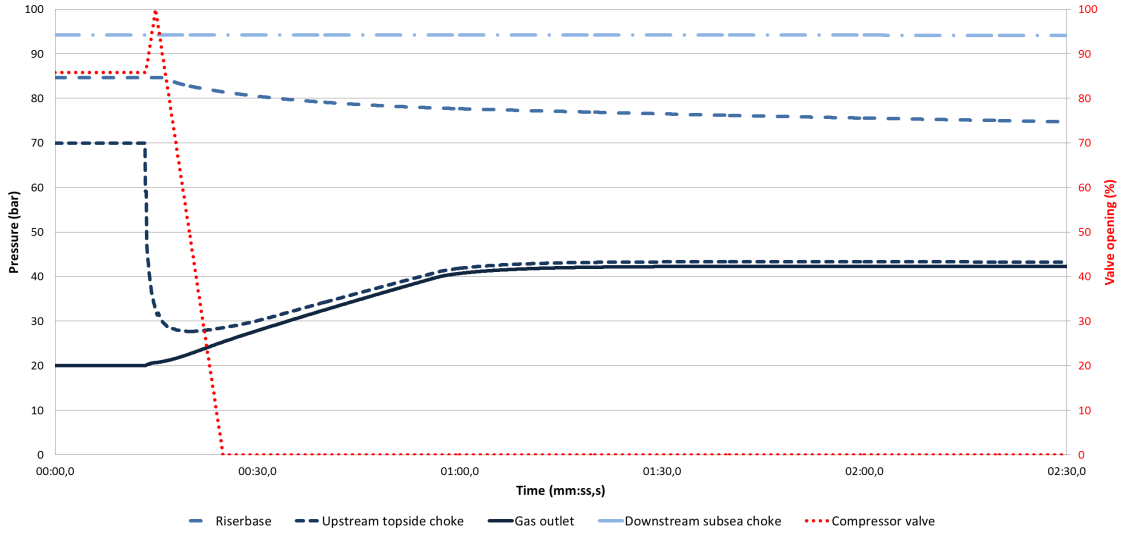

Figure B.4: Pressure for the choke collapse case B.

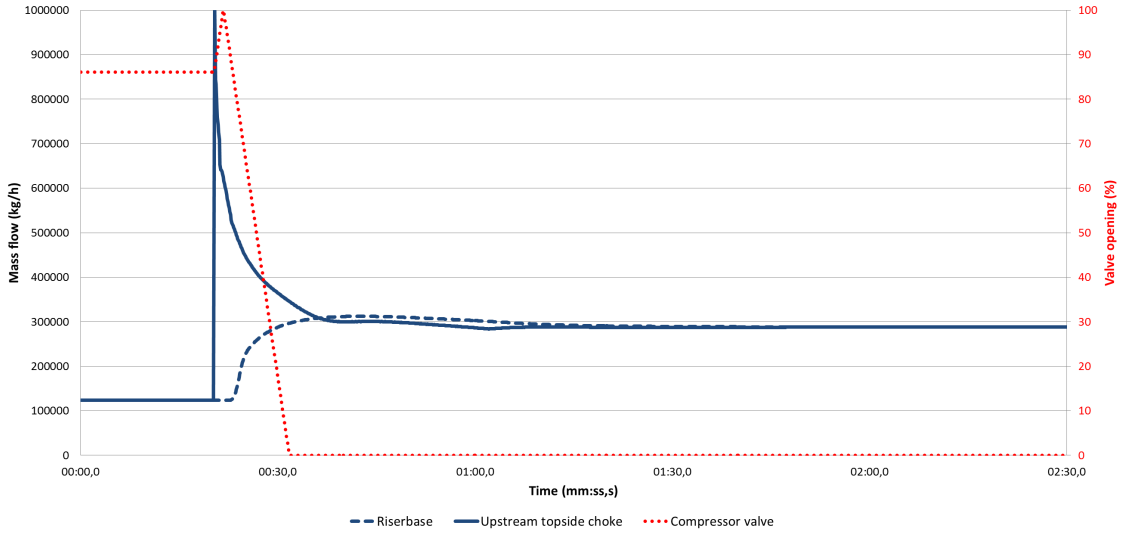

Figure B.5: Total mass flow rate for the choke collapse case C.

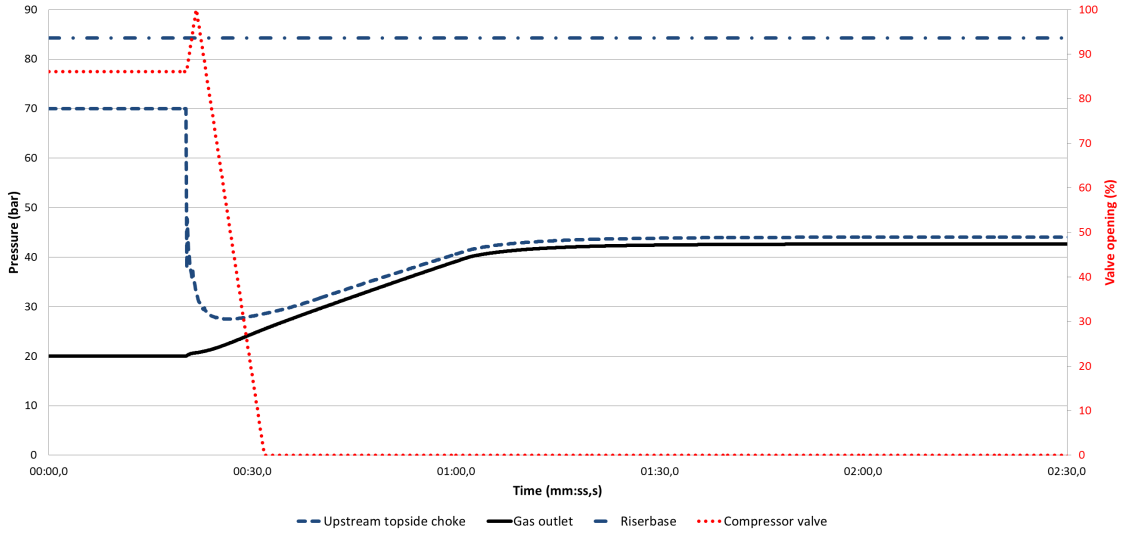

Figure B.6: Pressure for the choke collapse case C.

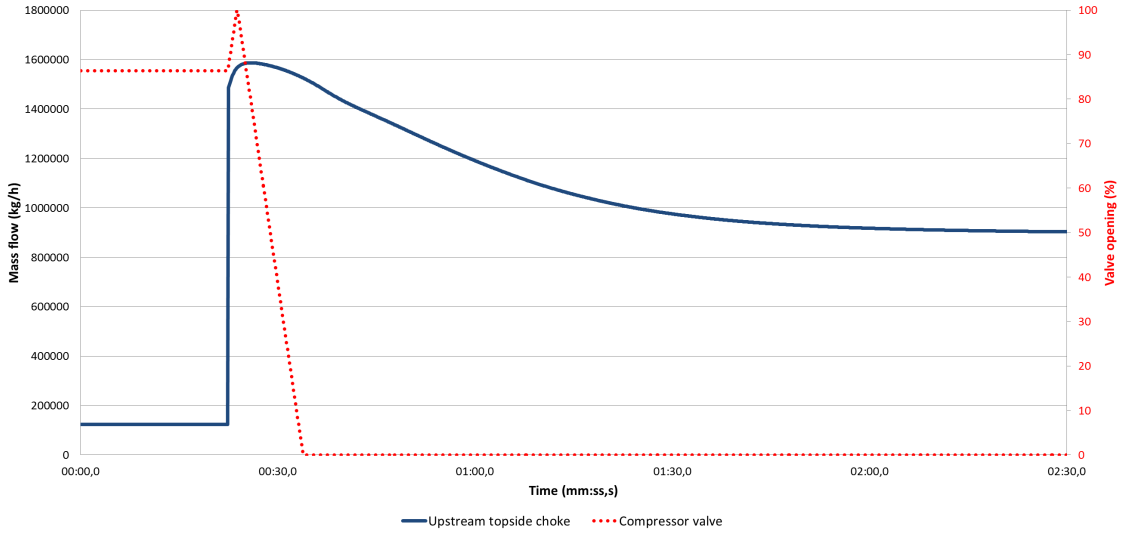

Figure B.7: Total mass flow for the choke collapse case D.

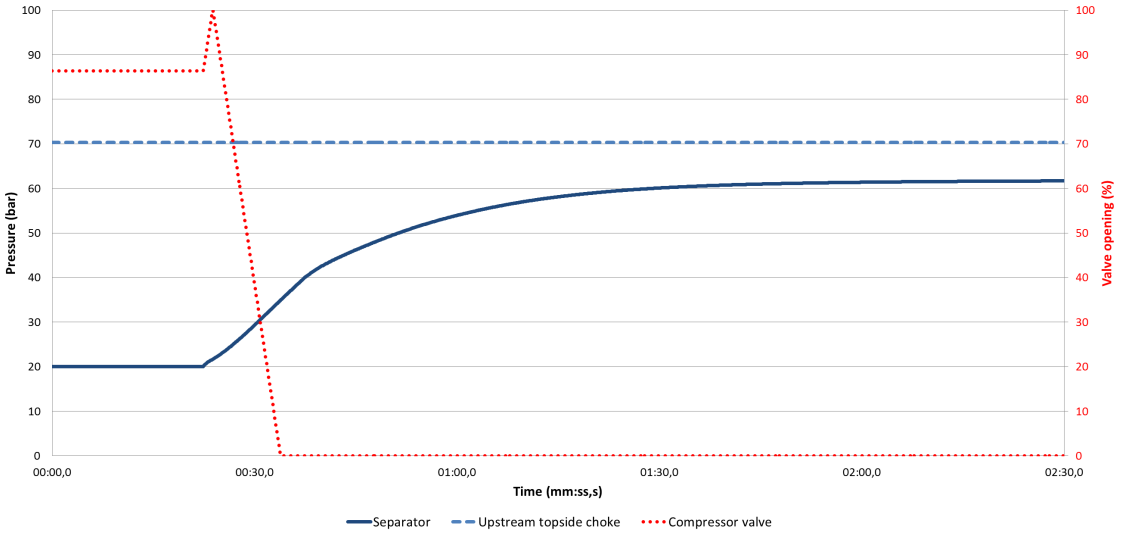

Figure B.8: Pressure for the choke collapse case D.

C Appendix C

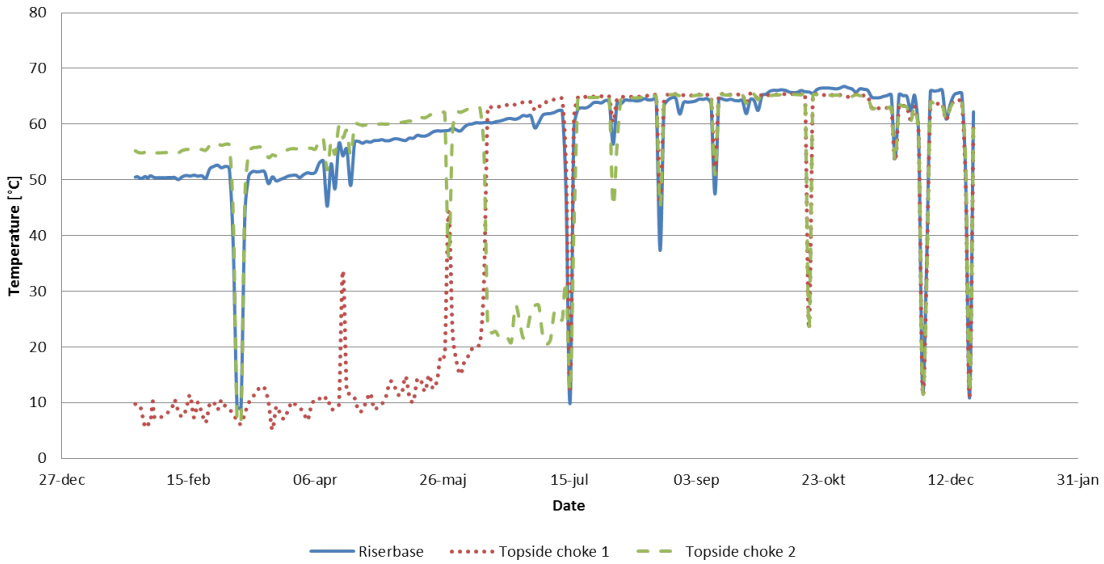

Figure C.1: Temperature profiles for the temperature meter by the riserbase and by each topside choke. Measurements shown for one production year, starting with validation case I and ending with validation case III.